4

Asymmetric Induction in Enantioselective Catalysis

4.1 Transmission of Asymmetry. 115
4.1.1 C_2- vs. Non-C_2-Symmetric Catalysts 116
4.1.2 Quadrant Diagrams 117

4.2 Chiral Metal Complexes from Chiral Ligands. 118
4.2.1 Bis(oxazolines) 118
4.2.1.a Control of Nucleophile Trajectory by Chiral Ligands. 119
4.2.1.b Indirect Control of Nucleophile Trajectory via Substrate Relay 121
4.2.2 BINOL-Based Lewis Acids 123

4.3 Asymmetric Induction with Chiral Metallocene Catalysts. 126

4.4 Transmission of Asymmetry to Substituents within a Metal–Ligand Adduct 128
4.4.1 Conformations of Chiral Metallacycles: BINAP and TADDOL 129
4.4.2 BINAP-Based Catalysts 129
4.4.3 TADDOL-Based Complexes 135

4.5 Environments from Ligands That Form Diastereotopic Complexes 140
4.5.1 Coordination of Diastereotopic Lone Pairs. 140
4.5.2 Binding of Diastereotopic Groups. 142

4.6 Electronic Asymmetry of Coordination Sites 143

4.7 Steric Bias of Configurationally Dynamic Ligand Stereocenters. 147
4.7.1 Ligands with Chiral Relay Groups Not Directly Connected to the Metal 147
4.7.2 Catalysts That Are Chiral at the Metal Center 149
4.7.3 Ligands That Can Adopt Atropisomeric Conformations 151
4.7.3.a Axial Chirality Induced in Backbone Biphenyl-Based Ligands . 151
4.7.3.b Axial Chirality Induced in Pendant Biphenyl-Based Ligands . . 153
4.7.3.c Axial Chirality Induced in Atropisomeric Amides. 155

4.8 Induced Asymmetry in the Substrate 156
4.8.1 Diastereomeric Complexes with Prochiral Substrates 156
4.8.2 Substrates with Chiral Relays 157
Concluding Remarks 158
References 160

One of the most important goals of asymmetric catalysis is the rational design and optimization of new catalysts. Although this seems like a straightforward exercise, it is far from it. Our understanding of the structure and function of catalysts, and the mechanisms of asymmetric reactions, is rudimentary. Although the lack of emphasis on mechanistic studies is certainly a contributing factor, it is often found that the reaction mechanisms are considerably more complex than anticipated. Furthermore, the difference in energy between diastereomeric transition states ($\Delta\Delta G^{\ddagger}$), which lead to enantiomeric products, is often small, complicating rational catalyst optimization. Given these challenges, it is not surprising that most catalyst optimization is performed with a combination of rational design, chemical intuition, and serendipity.

To understand how asymmetry is transmitted from the catalyst to the substrate, it is necessary to know the three-dimensional structure of the ligated catalyst. This is particularly challenging if the ligand retains a high degree of conformational flexibility when bonded to the metal, because it is more difficult to determine the conformation of the ligand in the transition state. For these reasons, it is easiest to begin studying the transmission of asymmetry in catalysts where the ligand–metal adduct has little rotational freedom.

This chapter examines how different types of chiral catalysts transmit asymmetry in enantioselective reactions. Emphasis is initially placed on ligands and catalysts that are well-defined. As the chapter progresses, and catalysts with additional degrees of conformational flexibility are introduced, the proposed structures and transition states are more speculative. Nonetheless, much can be learned from such systems.

4.1 Transmission of Asymmetry

In many cases asymmetric catalysts often bind and react preferentially with one of the prochiral faces of the substrate. In others, asymmetric catalysts bind the substrate and shield one of the prochiral faces, thus impeding reaction at that face. Despite the simplicity of these strategies, the mechanics of transmission of asymmetry from the catalyst to the substrate are complex and not well-understood in many systems. Furthermore, there are many classes of chiral ligands and catalysts, and the nature of

asymmetry transmission from the catalyst to the substrate varies greatly. Thus, this section first introduces some of the means by which the asymmetry of the catalyst is transmitted to the substrate.

The most common method to transfer asymmetry from a catalyst to the substrate relies on steric biasing. Other catalyst–substrate interactions, such as π-interactions between aromatic groups on the catalyst and substrate, or hydrogen bonding between the catalyst and substrate, etc., can also play important roles and may be used in combination with steric biasing (see Chapter 5).

4.1.1 C_2- vs. Non-C_2-Symmetric Catalysts

C_2-Symmetric catalysts have received much attention and merit special consideration in the context of the transmission of asymmetry. In the early days of asymmetric catalysis, it was often observed that catalysts containing C_2-symmetric ligands were, in general, more enantioselective than those with non-C_2-symmetric ligands. It was proposed that this selectivity resulted from the smaller number of metal–substrate adducts and transition states available to these catalysts than are available to catalysts containing less-symmetric ligands.[1–3] This principle is illustrated in the context of the asymmetric allylation reaction in **Figure 4.1**. The most common mode of nucleophilic attack on η³-allyl is on the face opposite the bulky palladium center.[4,5] Recall that interconversion of the diastereomeric intermediates occurs within the coordina-

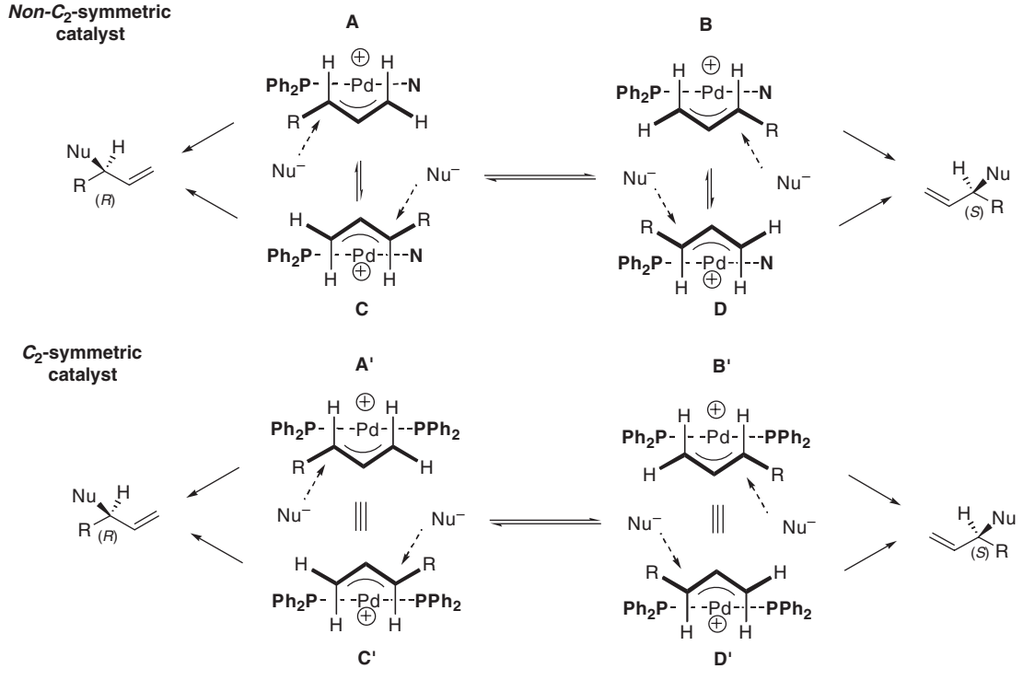

Figure 4.1. Palladium π-allyl complexes with a non-C_2-symmetric P–N ligand and a C_2-symmetric P–P ligand illustrating the number of diastereomeric lowest-energy transition states for nucleophilic attack. The chiral ligand backbone and the Pd–allyl bond are omitted for clarity.

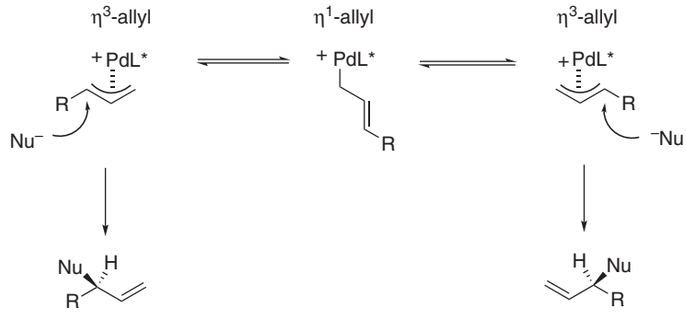

Figure 4.2. Interconversion of diastereomeric palladium–allyl complexes. The interconversion may be assisted by coordination of an additional ligand.

tion sphere of the metal center.[6] This interconversion of diastereomeric intermediates proceeds by reversible generation an η^1-allyl species in a mechanism often described as a π–σ–π interconversion (**Figure 4.2**). The interconversion can be aided by coordination of an additional ligand, as will be seen in subsequent chapters.

Catalysts containing P–N ligands can bind either of the two prochiral faces of an allyl group (**Figure 4.1**, where the chiral ligand backbone and the bond between the allyl and palladium are omitted for clarity). Attack of a nucleophile, such as phenoxide, can occur pseudotrans to phosphorus or pseudotrans to nitrogen in intermediates **A** and **C**, respectively, to generate the (*R*)-product (**Figure 4.1**, top). These two modes of attack are both sterically inequivalent and electronically distinct (due to the trans effect).[7] Likewise, attack on diastereomers **B** and **D** can give rise to formation of the (*S*)-product. In contrast, when a C_2-symmetric catalyst is employed, the transition states for attack on intermediates **A'** and **C'** are equivalent, as are **B'** and **D'**. Thus, the number of competing diastereomeric transition states is reduced with C_2-symmetric catalysts, simplifying analysis and catalyst design. The simplification is even greater in five- and six-coordinate intermediates, where the number of diastereomeric metal–ligand adducts is greater (see Figure A.8). Some examples of C_2-symmetric bis(phosphines) and non-C_2-symmetric P–N ligands are illustrated in **Figure 4.3**. Although many catalysts lacking C_2-symmetry exhibit high levels of enantioselectivity, those containing C_2-symmetric ligands comprise one of the most important and selective classes of catalysts.

4.1.2 Quadrant Diagrams

A generic model for steric biasing of chiral metal–ligand adducts has been advanced to facilitate the prediction of the facial stereoselectivity in catalyst–substrate complexes and transition states. In this model, the environment around the metal is divided into quadrants in which the horizontal dividing line is congruent with a plane or pseudoplane in the catalyst. For simplicity, the quadrant diagram is given for a C_2-symmetric catalyst (**Figure 4.4a**). The two shaded diagonal quadrants represent space that is occupied by substituents on the ligand that extend forward, whereas the unshaded rectangles correspond to less-occupied space. Binding of the prochiral faces of an olefin to a metal, for example, would give rise to diastereomers in which the

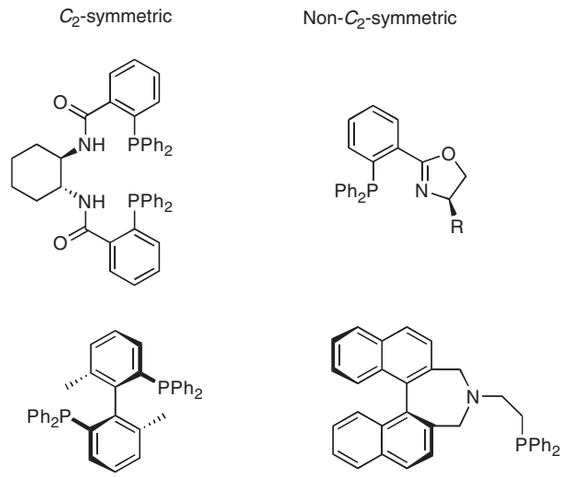

Figure 4.3. Examples of C_2-symmetric bis(phosphines) and non-C_2-symmetric P–N ligands used in catalytic asymmetric allylation reactions.

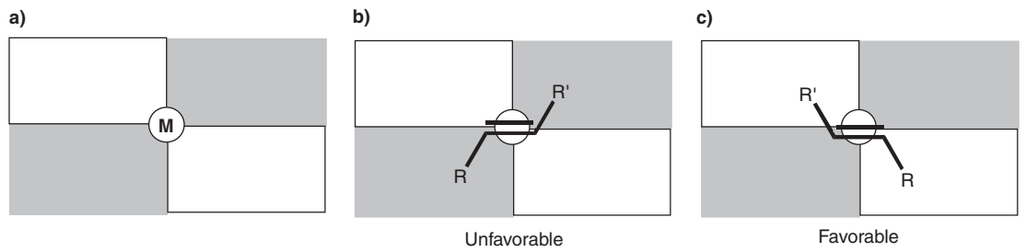

Figure 4.4. a) Quadrant diagrams for a C_2-symmetric catalyst. The shaded regions represent quadrants occupied by substituents on the ligand and the unshaded sections correspond to relatively unoccupied areas. b) Unfavorable binding and c) favorable binding of an olefin in diastereomeric olefin complexes.

more-stable diastereomer contains the R and R′ substituents positioned in the open, unshaded quadrants (**Figure 4.4b** vs. **Figure 4.4c**).

The means by which metal complexes of chiral ligands block quadrants depends on the nature of the ligand and the metal–ligand adduct. In some cases, the ligands possess stereogenic centers in close proximity to the metal. In other cases, the stereogenic centers are located so far from the metal it is not obvious how the effect of these distant stereocenters can be transmitted to the site of reaction. We describe examples of each of these in the following sections.

4.2 Chiral Metal Complexes from Chiral Ligands

4.2.1 Bisoxazolines

Two popular families of ligands that provide rigid chiral environments on coordination are the C_2-symmetric bisoxazoline ligands,[8,9] such as Box and PyBox, and the semicorrin ligands.[10] The structures of these ligands and their coordination complexes

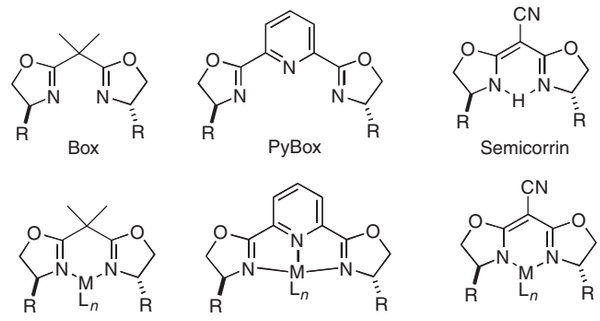

Figure 4.5. Structures of the bis(oxazoline) ligands, Box and PyBox and a semicorrin ligand, along with their metal complexes.

are shown in **Figure 4.5**. In conjunction with a variety of main-group and transition metals, these ligands form highly enantioselective catalysts that have been successfully used in many asymmetric reactions,[8–10] including the aldol, cyclopropanation,[11,12] aziridination,[13] Diels–Alder,[14,15] Michael,[16] and ene reactions.[17] The nearly planar metallacycle formed on binding the bidentate ligand, and the presence of the pendent five-membered rings, limit the flexibility of these ligand systems. The common feature of the ligands in **Figure 4.5** is that the substituents at the stereogenic centers extend forward, positioning them in close proximity to the metal center and the substrate binding sites. As will be illustrated below, the well-defined asymmetric environment of these ligands facilitates use of quadrant diagrams. Electronically, the anionic nature of the semicorrin ligands makes them stronger electron donors than the neutral bisoxazoline ligands. As a result, complexes of the semicorrin ligands are less Lewis acidic and will exhibit stronger binding of the chiral ligand.

4.2.1.a Control of Nucleophile Trajectory by Chiral Ligands

Several successful asymmetric transformations have been developed using chelating substrates in combination with copper(II)–bisoxazoline complexes, creating well-defined substrate–catalyst adducts that allow for more efficient catalyst optimization.[8] The crystal structure[15] of [(*S*,*S*)-*t*-Bu-Box)]Cu$(OH_2)_2(SbF_6)_2$ shown in **Figure 4.6**

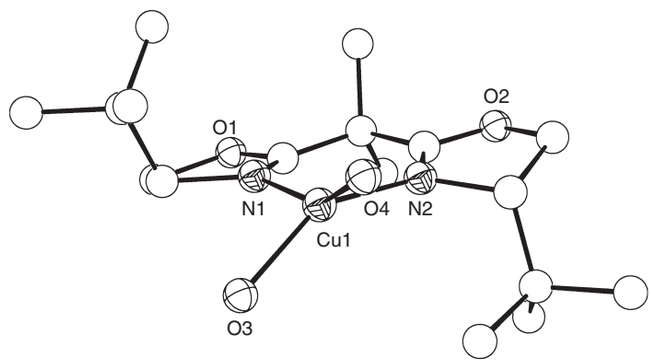

Figure 4.6. Structure of [(*S*,*S*)-*t*-Bu-Box)]Cu$(OH_2)_2(SbF_6)_2$, illustrating the distorted square-planar geometry of the copper and the ligand environment.

illustrates the pseudo-square-planar geometry of the Jahn–Teller-distorted d^9-copper center.[18] The SbF_6 counterions are not interacting with the copper center, and are not shown in the figure. The [(*S,S*)-*t*-Bu-Box]Cu^{2+} catalyst has proven particularly effective in the asymmetric Diels–Alder reaction with chelating imide dienophiles (**Equation 4.1**),[15] which prefer the *s*-cis conformation when coordinated (**Figure 4.7**).

Equation 4.1

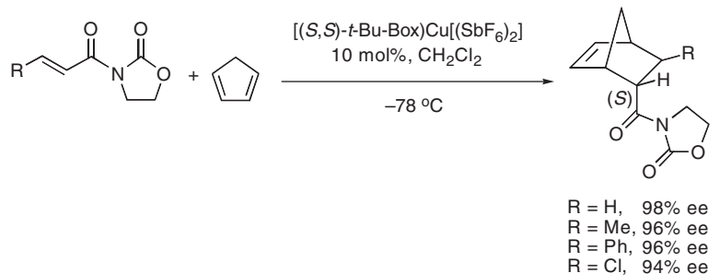

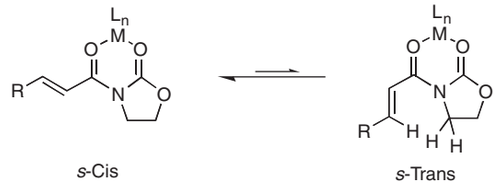

Figure 4.7. The *s*-cis conformation of the dienophile is strongly favored over the *s*-trans conformer when bound in a bidentate fashion.

Semiempirical calculations of copper(II) (Box)Cu(sub)$^{2+}$ complexes (where sub = bidentate dicarbonyl substrate) suggest a similar degree of distortion from square-planar geometry to that observed in the structure of [(*S,S*)-*t*-Bu-Box)]Cu$(H_2O)_2^{2+}$ in **Figure 4.6**.[14] To simplify the understanding of the stereochemical outcome of the reaction (**Equation 4.1**), the nearly planar backbone of [(*S,S*)-*t*-Bu-Box)]Cu^{2+} is represented by a horizontal line with the protruding substituents extending forward (**Figure 4.8**). Upon coordination of the imide substrate to [(*S,S*)-*t*-Bu-Box)]Cu^{2+}, the

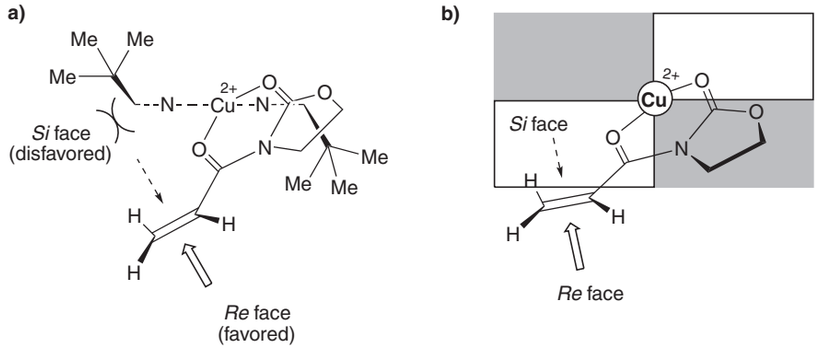

Figure 4.8. Proposed models for the stereochemical control in the Diels–Alder reaction. a) The bisoxazoline ligand is represented by the horizontal line and protruding *t*-Bu groups. b) A quadrant diagram for the same facial selectivity.

prochiral faces of the dienophile are in distinctly different steric environments, with the *Si* face (i.e., the *Si* face of the alkene) blocked by the protruding *t*-Bu group of the *t*-Bu-Box ligand. Attack of the diene, therefore, takes place at the less-hindered *Re* face with excellent enantioselectivities (**Equation 4.1**).[19] This model for facial selectivity with bis(oxazoline) can be applied to several asymmetric reactions involving chelating dicarbonyl substrates and the (Box)Cu^{2+} family of catalysts, provided that the copper geometry is close to square-planar in the catalyst–substrate adducts.

When using such a model for bisoxazoline-based catalysts, caution must be exercised, because changes in metal geometry or coordination number will impact the enantioselectivity. For example, substitution of Cu(II) for its neighbor Zn(II) forming [(*S,S*)-*t*-Bu-Box)]Zn$(SbF_6)_2$, resulted in formation of the opposite enantiomer of the product in 56% ee (**Equation 4.2**). Likewise, the same facial selection was observed for [(*S,S*)-Ph-Box)]Zn$(SbF_6)_2$, which gave the product in 92% ee. In changing the metal geometry from distorted square-planar (Cu^{2+}) to tetrahedral (Zn^{2+}), the *Re* face is now shielded (**Figure 4.9**), in contrast to the Cu(II) complex (**Figure 4.8**).[20] Furthermore, switching to the magnesium catalyst, which is also proposed to have the tetrahedral geometry, again gives the (*R*) enantiomer.[21] It is also noteworthy that the Fe(III)–bis(oxazoline) catalysts, which are likely octahedral, gave the same stereochemistry as the Zn(II) and Mg(II) complexes.[21]

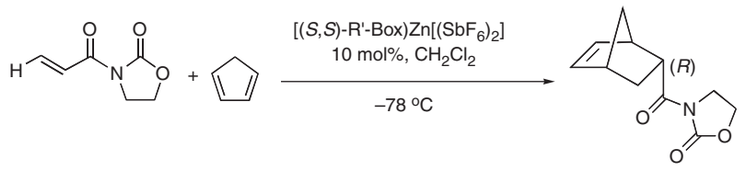

Equation 4.2

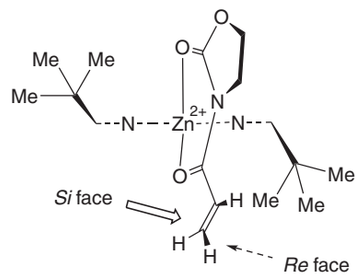

Figure 4.9. Proposed model for the stereochemical control in the Diels–Alder reaction. The bisoxazoline ligand is represented by the horizontal line and protruding *t*-Bu groups.

4.2.1.b Indirect Control of Nucleophile Trajectory via Substrate Relay

Analysis of the stereochemical outcome of a reaction with bis(oxazoline)-based catalysts becomes more difficult when the trajectory of the attacking nucleophile is parallel to the plane defined by the nitrogens of the ligand and the metal center. An

interesting example of this behavior arises in the Tsuji–Trost asymmetric allylic-alkylation reaction.[22,23] The key steps and intermediates are shown in **Figure 4.10**. Reaction of either enantiomer of the allylic-acetate with a (Box)Pd(0) intermediate leads to formation of a η^3-allyl complex. The nucleophile, $KCH(CO_2Me)_2$, attacks the η^3-allyl termini from the face opposite the palladium. In the presence of the chiral bisoxazoline ligand, the nucleophile preferentially attacks one of the two termini-leading to the major enantiomer, while the minor enantiomer, is generated by attack at the other terminus.

Insight into the factors that control the regioselectivity of the nucleophilic attack and, therefore, the enantioselectivity, were gleaned from X-ray crystallographic studies of $[(Box)Pd(\eta^3\text{-allyl})]^+$ derivatives. In the structure of the parent cation, $[(Bz\text{-}Box)Pd(allyl)]^+$, the palladium has the expected square-planar geometry and the (Bz-Box)Pd metallacycle is nearly planar (**Figure 4.11**). In contrast, in the structure of the intermediate, $[(Box)Pd(1,3\text{-diphenylallyl})]^+$, there are significant nonbonded interactions between a benzyl substituent of the ligand and the adjacent phenyl group of the η^3-allyl. To minimize the steric repulsion between these groups, the metallacycle has distorted markedly from planarity, as depicted in **Figure 4.11**. Furthermore, there is a lengthening of the Pd–N and Pd–C bond lengths associated with these interacting groups (**Figure 4.11**).

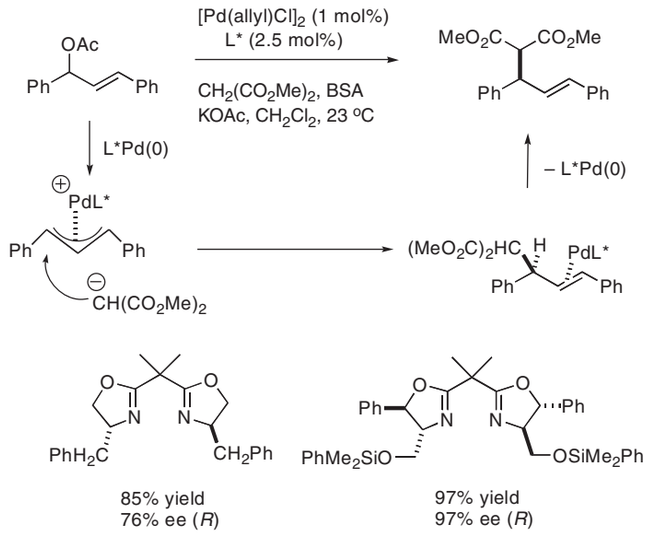

Figure 4.10. The mechanism of the asymmetric allylation reaction (BSA = bissilylacetamide).

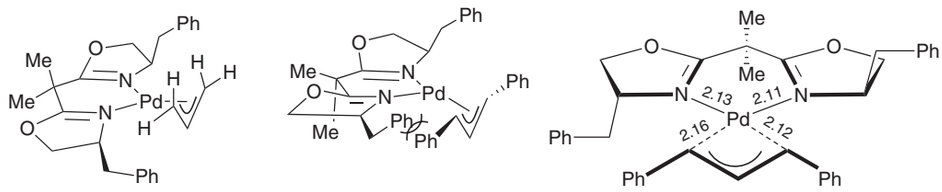

Figure 4.11. Drawings of $(Bz\text{-}Box)Pd(allyl)^+$ and $(Bz\text{-}Box)Pd(1,3\text{-diphenylallyl})^+$ based on the X-ray crystal structures. Bond distances are in angstroms (Å).

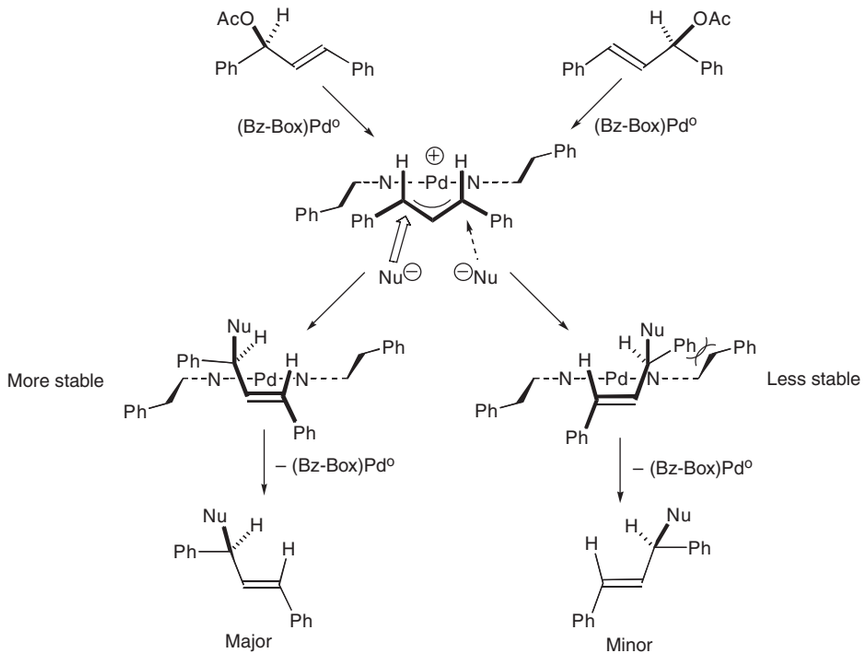

Figure 4.12. Model for stereoselection in the asymmetric allylation reaction. Attack of the nucleophile at the elongated C–Pd bond leads to the less-strained olefin complex.

Based on the configuration of the product formed on reaction of [(Bz-Box)Pd(1,3-diphenylallyl)]$^+$ with the nucleophile, attack has occurred on the allyl terminus with the elongated Pd–C bond. It has been suggested that attack at the more crowded position is favored. As the reaction occurs, the forming carbon–carbon double bond rotates into the plane containing the Pd and nitrogen atoms of the ligand (**Figure 4.12**). Attack at the more-hindered position results in a reduction of nonbonded interactions in the transition state leading to the palladium–olefin complex.[10] Inspection of the proposed geometries of the olefin products highlights the differences in stability of the diastereomeric products (**Figure 4.12**). The idea that the regioselectivity of the nucleophilic attack is controlled by the interaction of the bound substrate with the ligand can be contrasted with the more commonly invoked rational for asymmetric induction, which involves direct interaction of the nucleophile with the chiral ligand.

4.2.2 BINOL-Based Lewis Acids

An important class of "privileged ligands" is based on the parent atropisomeric BINOL (1,1′-bi-2-naphthol) (**Figure 4.13**).[24] BINOL is fairly stable to racemization because of the steric hindrance to rotation about the pivotal 1,1′-bond. Barriers to racemization of BINOL have been determined to be 37–38 kcal/mol.[25,26] No racemization was detected on heating to 100 °C in a dioxane/water mixture for 24 h, although addition of strong acid or base will cause racemization at this temperature.[26] BINOL derivatives bind well to many main-group, transition-metal, and lanthanide

compounds to form catalysts that exhibit exceptionally high levels of enantioselectivity.[27–30] On binding to metals, the BINOLate ligand forms a rigid chiral metallacycle. **Figure 4.14** illustrates the skewed conformation of the BINOLate metallacycle viewed from the O–M–O plane.

Numerous highly enantioselective catalysts employ the parent BINOL ligand. In addition, many BINOL derivatives have been introduced and used successfully in asymmetric catalysis.[27–29,31] In understanding how asymmetry is conveyed in BINOLate-based catalysts, it is easiest to examine systems substituted at the 3,3′-positions, because the substituents typically extend in the direction of the substrate binding site (see below). In contrast, the hydrogens at the 3,3′-positions of the parent BINOLate ligand do not protrude into the metal binding site (**Figure 4.14**). Consequently, the transfer of asymmetry with BINOLate-based catalysts is poorly understood. It is possible that the skewed conformation of the BINOLate ligand causes an electronic asymmetry at the metal center that influences the transfer of asymmetry by controlling the orientation of substrate binding (see Section 4.6).[32] Also complicating our understanding of how the BINOLate ligand functions is the fact that many BINOLate-based catalysts involve early transition metals, such as titanium or zirconium, or lanthanides. In these systems, the metal coordination number and aggregation state

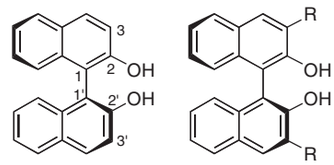

Figure 4.13. Structures of the parent BINOL and common derivatives substituted at the 3,3′-positions.

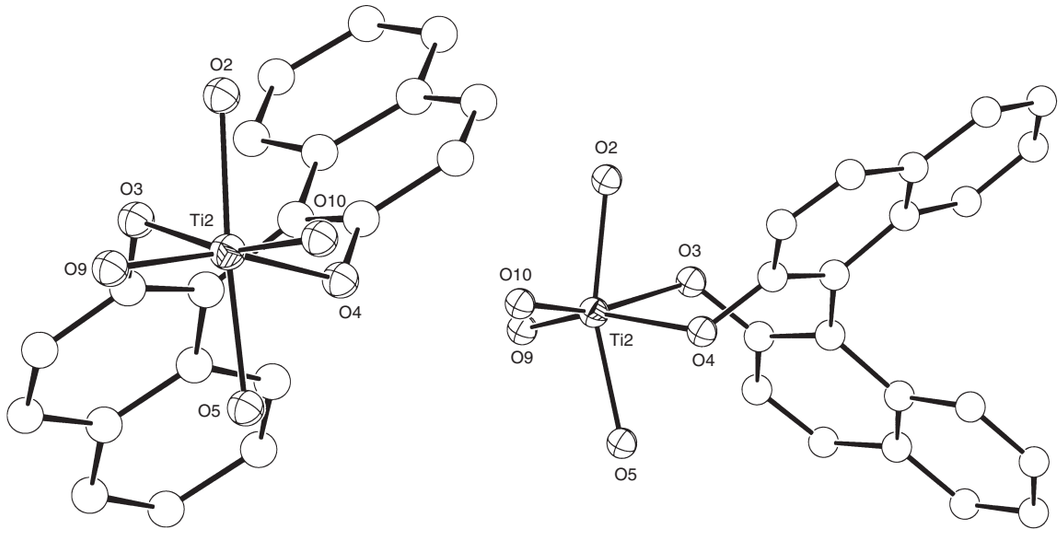

Figure 4.14. Patrial structure illustrating the skewed conformation of the BINOLate metallacycle bound to a pseudo-octahedral titanium center.

are often unknown. Thus, to simplify the discussion of asymmetric induction with BINOLate ligands, we will employ a stoichiometric Lewis acid based on boron. Boron compounds of this type are known to be tetrahedral, and as such, are monomeric.

A series of boron Lewis acids bearing ligands derived from BINOL were prepared for the Diels–Alder reaction with peri-hydroxyquinones (**Figure 4.15**).[33,34] The peri-hydroxyquinone substrates chelate to boron, limiting the conformational flexibility of the substrate–Lewis acid adduct. The enantioselectivity in the cycloaddition reaction will be controlled by the ability of the 3,3′-substituents on the BINOL to shield one of the prochiral faces of the dienophile. Thus, when the 3,3′-dimethyl-BINOL ligand was utilized (R = Me, **Figure 4.15**), the enantioselectivity of the anthraquinone product was 70%.[33] Use of the 3,3′-diphenyl BINOL (R = Ph), in which the phenyl substituents project further forward, better shielding one face of the dienophile, gave > 98% ee of the product.[33] The stereochemical outcome can be understood by examination of the drawings in **Figure 4.16**. Although there is no structural information on 3,3′-diphenyl-BINOLate complexes of boron, a partial structure of this ligand bonded to a tetrahedral metal center is shown. From these views it can be seen that the phenyl groups

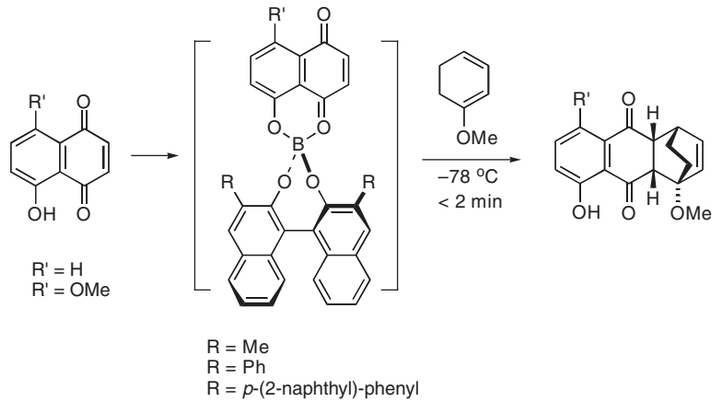

Figure 4.15. Asymmetric Diels–Alder of peri-hydroxyquinone promoted by BINOLate–boron Lewis acids.

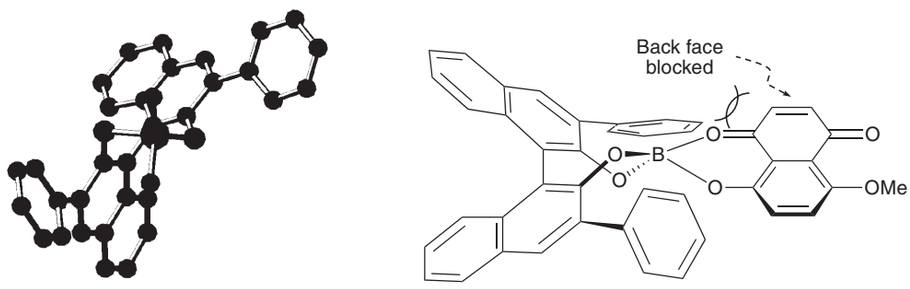

Figure 4.16. Partial structure illustrating the skewed conformation of the 3,3′-diphenyl-BINOLate ligand bound to a tetrahedral metal center (left). The same (Ph_2-BINOLate)B fragment viewed from a different angle, with the substrate added (right). The back face of the reactive double bond is rendered inaccessible by the distant phenyl group.

block adjacent quadrants, leaving two quadrants open. Upon binding of the substrate, the distant phenyl group shelters the reactive double bond from attack on the back face, while the front face is exposed, allowing the reaction to take place.

This Diels–Alder reaction was employed in the synthesis of (+)-diepoxin σ, which possesses antifungal, antibacterial, and antitumor activity.[34] The dieneophile was the peri-hydroxyquinone, where R′ = OMe, and the diene was cyclopentadiene, which is smaller than the 2-methoxy cyclohexadiene used to generate the anthraquinone derivative in **Figure 4.15**. As a result, the 3,3′-diphenyl-BINOL-based system did not exhibit the same degree of steric bias and gave low ee. Further extending the length of the 3,3′-substituents was found to improve enantioselectivity. Thus, when R = *p*-(2-naphthyl)phenyl, the enantioselectivity increased to 93%.

4.3 Asymmetric Induction with Chiral Metallocene Catalysts

Chiral group IV metallocenes have been found to polymerize terminal olefins with a high degree of stereocontrol over the polymer architecture.[35] It is not surprising, then, that resolved versions of these metallocenes have also been successfully applied in asymmetric catalysis.[36] The chiral ligand scaffolding around the metal center in the ansa-metallocene catalysts is conformationally limited by the ethylene tether, and therefore, fairly well-defined. This characteristic facilitates prediction of the sense of enantioselection in the reactions of these C_2-symmetric complexes. The most commonly applied ansa-metallocenes in asymmetric catalysis are based on group IV metals and ethylene-1,2-bis(η^5-4,5,6,7-tetrahydro-1-indenyl), abbreviated EBTHI (**Figure 4.17**).[36,37]

An example of the use of such ansa-metallocene catalysts is the asymmetric reduction of imines to afford the corresponding amines. As little as 0.02 mol% catalyst can be used to generate amine products in high yields and enantioselectivities (**Figure 4.18**).[38–43] The silane employed in this reaction is typically phenylsilane (H_3SiPh) or a soluble polymer, polymethylhydrosiloxane (PMHS), with the repeat unit $[SiH(Me)O]_n$.[43]

The reaction is initiated by activation of (EBTHI)TiF_2 (0.5–5 mol%) with phenylsilane, methanol, and pyrrolidine. Under these conditions, an active titanium(III) hydride is likely formed.[38] As illustrated in **Figure 4.19**, the mechanism is postulated to

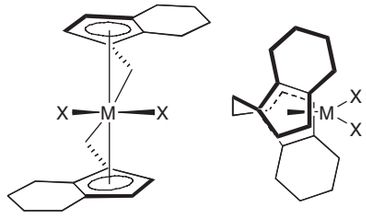

Figure 4.17. Two views of the chiral ansa-metallocene complex (EBTHI)MX_2.

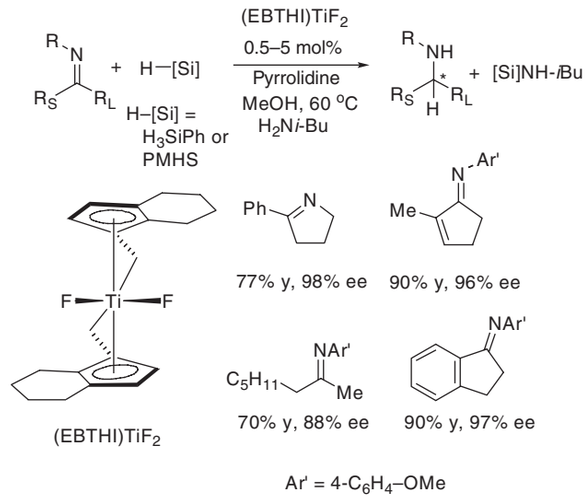

Figure 4.18. Asymmetric hydrosilylation of imines with (EBTHI)TiF_2 precatalyst (Ar′ = 4-C_6H_4-OMe).

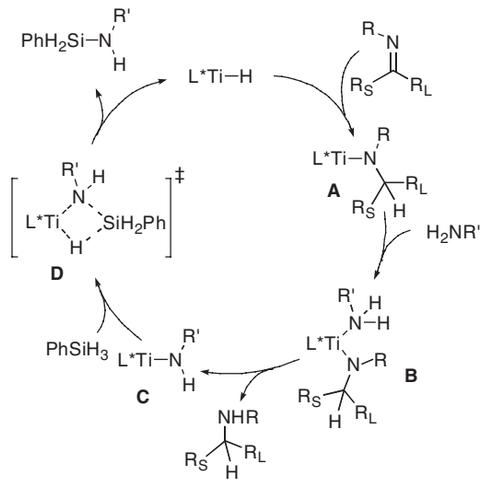

Figure 4.19. Proposed mechanism for the asymmetric hydrosilylation of imines.

proceed by enantioselective insertion of the prochiral ketimine into the titanium(III) hydride to generate a secondary amide (**A**). In the absence of added amine, cleavage of the intermediate amide **A** was the turnover-limiting step.[39] Slow addition of a primary amine, such as isobutylamine resulted in higher TOF, because the isobutylamine exchanges with the bulkier chiral amide to liberate the enantioenriched amine product. The sterically less-encumbering primary amide is more easily cleaved by the silane through a four-centered transition state[44] to regenerate the titanium hydride and form an equivalent of silylisobutylamine.

The model for asymmetric induction for this process is illustrated in **Figure 4.20**, where R_L and R_S are the large and small substituents on the ketimine.[40] Most ketimine substrates can have two isomeric forms, *syn* and *anti*, which give rise to four isomeric

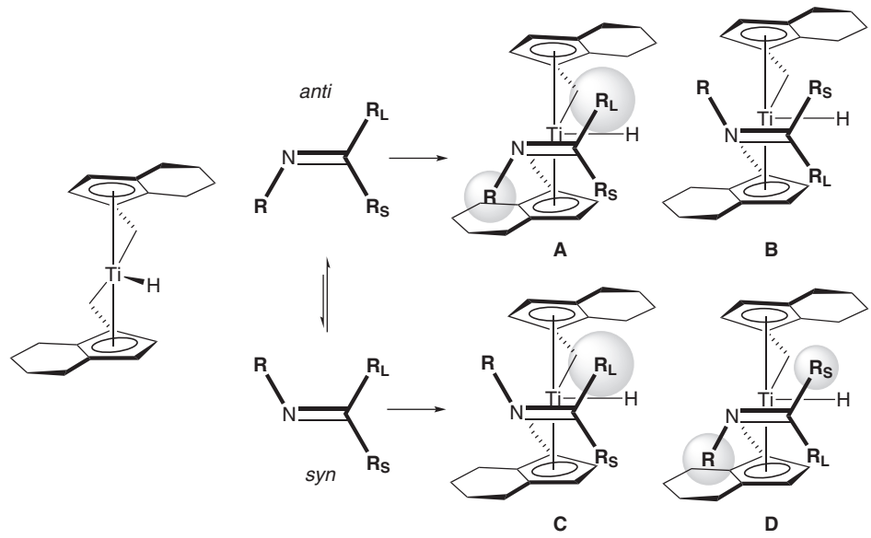

Figure 4.20. Proposed transition states for the asymmetric reduction of *anti* and *syn* ketimines. The spheres highlight steric clashing between the imine substituents and the catalyst.

transition states (**Figure 4.20**). In the transition states **A** and **B** with the *anti* isomer, **A** is destabilized, because interactions of R and R_L with the metallocene ring system. In contrast, in transition state **B** only R_S is directed toward the ligand. In the transition states with the *syn* ketimine, **C** is more favorable than **D**, which has both R_S and R interacting with the ligand. The stereochemistry of the products formed from cyclic ketimine, which proceed through the *syn* transition states, is consistent with this model.

With acyclic ketimines, reaction of the *anti* isomer is predicted to take place through transition state **B** and the *syn* isomer through transition state **C**. This dual-path reaction manifold may result in a decrease in the observed enantioselectivity, because these transition states give opposite configurations of the product. This does not appear to be a serious limitation, however. The aliphatic imine in **Figure 4.18** has an *anti*/*syn* ratio of 2.6:1, but undergoes reduction with an enantioselectivity of 88%.[43] This result suggests that the *syn* and *anti* ketimines equilibrate under the reduction conditions and the reaction proceeds primarily via transition state **B**.

4.4 Transmission of Asymmetry to Substituents within a Metal–Ligand Adduct

In the early days of asymmetric catalysis, it was thought essential to position the stereogenic center or centers of the ligand as close as possible to the reactive site on the metal.[45] Initial chiral phosphines were therefore prepared that were chiral at phosphorus, as exemplified by the ligand CAMP (**Figure 4.21**).[46] In hindsight, it is surprising that rhodium complexes of this ligand were fairly enantioselective, given the high

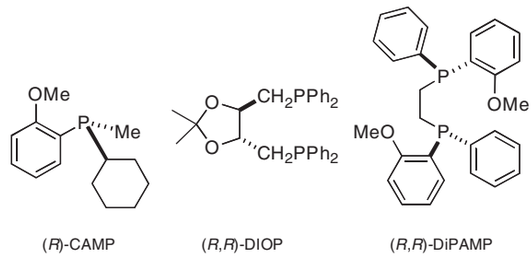

Figure 4.21. Important early chiral phosphine ligands.

degree of rotational freedom about the phosphorus–carbon and the rhodium–phosphorus bonds. When DIOP,[1,47] a chiral bidentate phosphine with two remote stereogenic centers (**Figure 4.21**), was introduced chemists began to appreciate the significant role that ligand conformations would play in enantioselective catalysis. The performance of catalysts based on DIOP inspired the development of the chelating ligand DiPAMP (**Figure 4.21**), which subsequently became the basis of a commercial synthesis of L-DOPA, a medication used in the treatment of Parkinson's disease.[45]

4.4.1 Conformations of Chiral Metallacycles: BINAP and TADDOL

Given the intense interest in asymmetric catalysis, it is not surprising that the synthesis and screening of new chiral ligands remains a very active area of research. Of the myriad enantioenriched ligands that have been employed in asymmetric catalysis, a few ligand classes seem to give consistently high levels of enantioselectivities with an array of metal centers. Because of the effectiveness of these ligands across a broad range of reactions, they have been referred to as "privileged ligands."[24]

4.4.2 BINAP-Based Catalysts

One of the prominent ligands in this class is the commercially available axially chiral BINAP (**Figure 4.22**).[48] This ligand is chiral, because of the skewed conformation of the binaphthyl rings, and it is stable to racemization due to the high barrier to rotation about the central C–C bond. Although best known for its application in catalytic enantioselective hydrogenations of olefins and ketones,[49,50] metal complexes of BINAP have found many applications in asymmetric reactions. BINAP can accommodate metals of different radii by rotating about the central aryl–aryl bond and the 2,2′-P–C

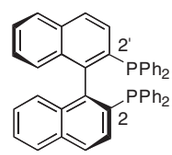

Figure 4.22. Structure of (*S*)-BINAP.

bonds, but once coordinated, the conformation of the ligand is constrained in the rigid metallacycle.

The efficiency with which BINAP-based catalysts transmit asymmetry to substrates results from transmission of the binaphthyl backbone axial chirality to control the position and orientation of the diastereotopic phenyl substituents. The skewed conformation of the seven-membered metallacycle is chiral and is set by the binaphthyl axial stereochemistry. The phenyl groups assume pseudoaxial and pseudoequatorial positions, as can be seen in the X-ray crystal structure of the BINAP ligand bound to ruthenium (**Figure 4.23**).[51] A stereoview is illustrated in **Figure 4.24**. The pseudoequatorial phenyl rings extend forward past the metal center and the pseudoaxial phenyl groups orient away from the metal. BINAP derivatives, of which there are many, and several chiral bidentate phosphines (see below) display these characteristics, but do not exhibit such pronounced differences in the positions of the pseudoequatorial and pseudoaxial phenyl groups. It is the combination of the protruding equatorial phenyl groups and the degree of orientation of the axial phenyl groups away from the substrate binding site that is thought to be responsible for the exquisite enantiocontrol in this ligand system.[52] The fact that substituents in the *para* positions of the phenyl groups often impact the enantioselectivity of the catalyst is consistent with this hypothesis, although electronic effects may also be important.[53] Additionally, an edge-face (CH-π) interaction between the phosphorus-bound aryl groups contributes to the differentiation of the pseudoaxial and pseudoequatorial

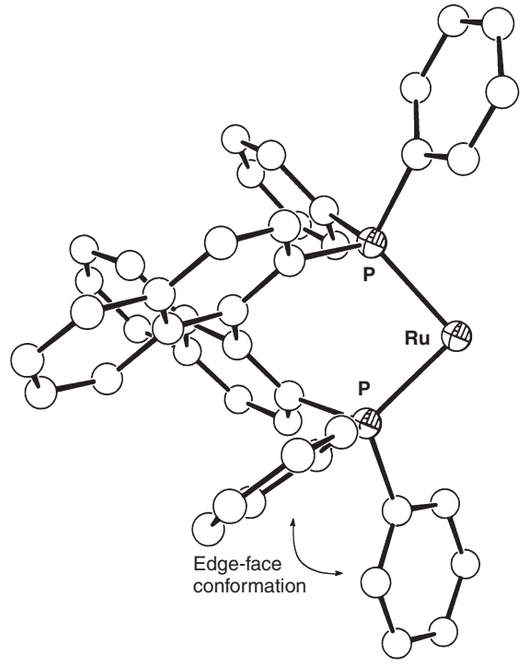

Figure 4.23. Partial structure of [(*S*)-BINAP)]Ru(O_2C-*t*-Bu)$_2$, with carboxylate ligands omitted for clarity. The pseudoequatorial phenyl rings are thrust forward, while the pseudoaxial phenyls are oriented away from the ruthenium center.

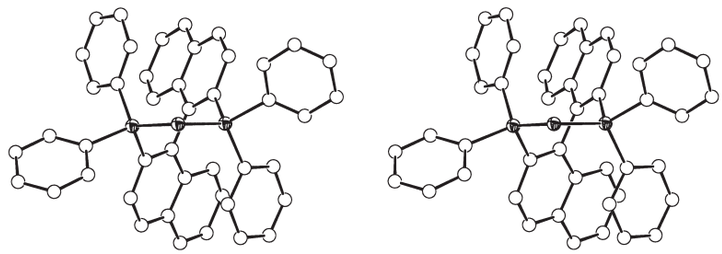

Figure 4.24. Stereoview of the metal–BINAP core from Figure 4.23, illustrating the chiral environment of the ligand.

phenyl groups. As such, the equatorial phenyl groups protrude with the face of the aryl forward. This important interaction can be seen in the structure in **Figure 4.23** and in the stereoview in **Figure 4.24**.[54,55]

To understand the control of asymmetry in catalysts bearing the BINAP ligand, the enantioselective hydrogenation reaction with the precatalyst (BINAP)Ru(O_2CR)$_2$ from **Figure 4.23** will be examined. The resultant catalyst exhibits high enantioselectivity with a wide range of substrates.[56] Detailed investigations of this system have led to an understanding of the reaction mechanism,[57] which is believed to proceed through a mono-hydride intermediate, and the proposal of a reliable model for the asymmetric induction.[57,58]

As documented in many examples, the best substrates for the asymmetric hydrogenation with this catalyst possess a pendant Lewis basic site that, along with the functional group undergoing reduction, binds to the ruthenium center, forming a chelate.[56,59] This is illustrated for one of the most important classes of substrates for this catalyst, the β-keto ester (**Equation 4.3**). Reduction of these substrates provides access to products analogous to those formed in aldol condensations. In the model for asymmetric induction, the ketone carbonyl is thought to coordinate in a π-fashion to the ruthenium, while the ester binds through an oxygen lone pair (**Figure 4.25**). Due to these different binding modes, the ketone component places greater steric demands on the ruthenium–BINAP system and occupies the least-hindered site on the catalyst, as shown in **Figure 4.25**. In the structure on the left, the interaction of the ketone with the protruding equatorial phenyl group of the BINAP, drawn in bold, destabilizes this diastereomer. In contrast, the right-handed structure places the ketone carbonyl in the quadrant with the axial P-phenyl group, which is directed away from the substrate. Here, it is assumed that the major diastereomer of the substrate–catalyst adduct will generate the major enantiomer of the product. This assumption, however, is not always valid.[60,61]

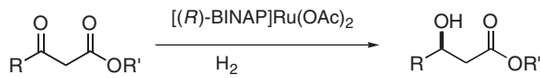

Equation 4.3

Another example involves the catalytic intramolecular hydroacylation of 4-pentenals with cationic rhodium catalysts containing bidentate chiral phosphines

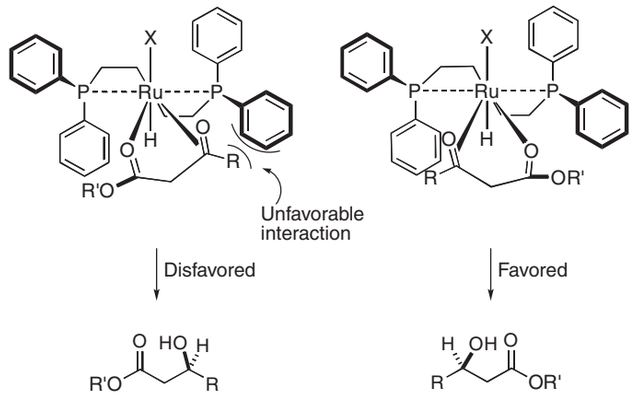

Figure 4.25. Proposed chelation of β-keto esters to the [(*R*)-BINAP]Ru moiety in the asymmetric hydrogenation (shown in Equation 4.3). The equatorial phenyl groups of the BINAP ligand are shown in bold. The unfavorable interaction of the ketone with the equatorial phenyl on the left destabilizes this diastereomer.

(**Equation 4.4**).[62–65] This reaction takes place at room temperature in acetone or methylene chloride with turnover numbers as high as 500, and isolated yields around 90%. The catalyst precursor, [(*S*)-BINAP)]Rh(NBD)ClO_4[48] (where NBD = norbornadiene), was briefly treated with hydrogen to prepare the catalyst, [(*S*)-BINAP)]Rh(sol)$_2ClO_4$ (where sol = solvent). Based on labeling experiments,[66–68] the mechanism is believed to involve initial oxidative addition of the acyl hydrogen. Like the ruthenium hydrogenation catalyst described above, the coordinatively unsaturated rhodium(III) intermediate possesses open coordination sites after the oxidative-addition step. Coordination of the pendent olefin with the C–C double bond situated roughly parallel to the Rh–H axis gives the proper alignment for the olefin insertion step (**Figure 4.26**). Binding of the olefin to the rhodium will occur to minimize steric interactions between the bound substrate and the equatorial phenyl groups. In the diastereomer on the left in **Figure 4.26**, the bulky *tert*-butyl group lies in the quadrant with the pseudoaxial phenyl group, which is directed away. In contrast, the other diastereomer results in severe steric interactions between the protruding pseudoequatorial phenyl group and the *tert*-butyl group, destabilizing this isomer. The next step in the mechanism is the olefin insertion and subsequent reductive elimination to generate the product with high enantioselectivity.[62]

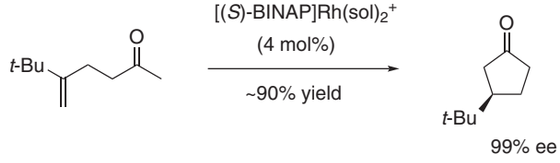

Equation 4.4

The quadrant model outlined in Section 4.1.2 has been used to facilitate the prediction of the facial stereoselectivity in reactions with catalysts bearing chiral bidentate phosphines (**Figure 4.27**). The protruding equatorial phenyl groups occupy the

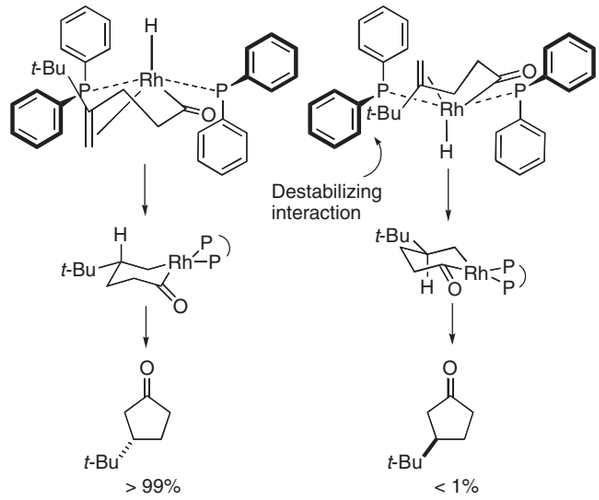

Figure 4.26. Diastereomeric binding modes of the unsaturated acyl substrate to the cationic [(*S*)-BINAP]Rh(H) moiety and cyclization. The equatorial phenyl groups are shown in bold.

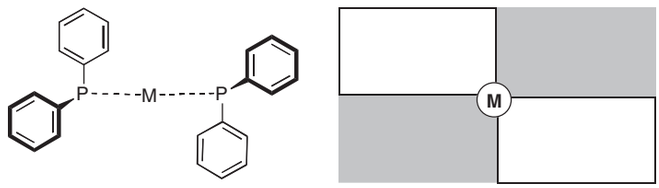

Figure 4.27. Model for the spacial positions of the ligand. The shaded regions are occupied by the pseudoequatorial phenyl groups (bold) that protrude forward.

two shaded diagram quadrants, blocking encroachment into these regions. The quadrants containing the pseudoaxial phenyl groups are unshaded. In order to minimize nonbonded interactions, the substrate avoids contact with the pseudoequatorial phenyl groups (i.e., the shaded regions of the model).

Other types of bidentate phosphine ligands exhibit a similar disposition of the phenyl substituents to BINAP. For example, the five-membered metallacycle formed on binding of (2*S*,3*S*)-bis(diphenylphosphino)butane [(*S*,*S*)-chiraphos, **Figure 4.28**] to metals adopts a twisted conformation. Although five-membered rings are normally conformationally flexible, the conformation of chiraphos is controlled by the methyl substituents on the ligand backbone, which are pseudoequatorially disposed in the lowest-energy conformation. The conformational twist of the metallacycle causes the phenyl groups to adopt pseudoaxial and pseudoequatorial positions (**Figure 4.28**). Based on structural information,[69] the pseudoequatorial and pseudoaxial phenyl groups of chiraphos are not as dissimilar in their positions when compared to those of BINAP.[70] As a result, the pseudoequatorial phenyl groups do not protrude to the same extent as they do in BINAP complexes, nor are the pseudoaxial phenyl rings of chiraphos directed away from the metal to the same degree. The sp^2 hybridized carbons

of the seven-membered metallacycle derived from BINAP induce a conformation that is more skewed than metallacycles with sp^3 hybridized carbons in the backbone, and thus create greater distinction between the axial and equatorial phenyl groups.

Both (*S*)-BINAP and (*S,S*)-chiraphos have been employed in the asymmetric acylation reaction in **Figure 4.29**. With simple substrates, where R = Me or *i*-Pr, both ligands exhibited the same sense of stereoselectivity, as would be expected by the models outlined in **Figures 4.27** and **4.28**. In these models, both ligands have the same twist sense, with the equatorial phenyl groups blocking the same quadrants (**Figure 4.27**). With bulky groups, such as *t*-Bu and $SiMe_3$, however, the (*S*)-BINAP- and (*S,S*)-chirophos-based catalysts give the opposite stereoselectivity (**Figure 4.29**). Assuming that the mechanisms are the same, the opposite facial selectivity suggests that the more-stable diastereomer of the acyl-hydride complex in the BINAP system becomes the less-stable diastereomer with the chiraphos catalyst.

Although the structures of the relevant intermediates are unknown, based on the ground-state crystal structures and the production of opposite enantiomers of the product with these catalysts, it has been suggested that the position of the axial phenyl groups in chiraphos, which are not directed away from the metal center to the same extent as in BINAP, cause greater steric interactions with the *t*-Bu group (**Figure 4.26**).[62] Admittedly, however, it is surprising that what is perceived to be a small difference in ligand conformation results in formation of the opposite enantiomer of the product.

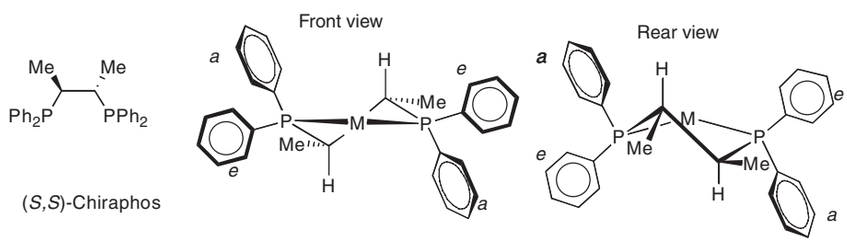

Figure 4.28. Front view of (*S,S*)-chiraphos with pseudoaxial (*a*) and pseudoequatorial (*e*) phenyl groups labeled.

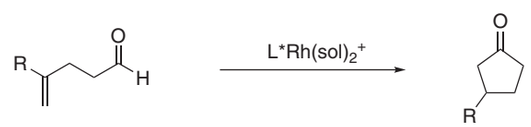

Entry	R	(*S*)-BINAP % ee (configuration)	(*S,S*)-chiraphos % ee (configuration)
1	Me	78 (*S*)	42 (*S*)
2	*i*-Pr	60 (*S*)	45 (*S*)
3	*t*-Bu	99 (*S*)	29 (*R*)
4	$SiMe_3$	99 (*S*)	8 (*R*)
5	CO_2*i*-Pr	99 (*S*)	11 (*R*)
6	CO*t*-Bu	94 (*S*)	63 (*R*)
7	COPh	94 (*S*)	64 (*R*)

Figure 4.29. Comparison of the enantioselectivities between BINAP and chiraphos catalysts in the hydroacylation reaction.

In examples with R = ketone or ester, it is possible that the carbonyl of the R group can undergo different secondary interactions with the (chiraphos)Rh- and (BINAP) Rh-based catalysts, resulting in formation of the opposite enantiomer. Comparisons of entries 1–4 in **Figure 4.29** serve as reminders that subtle differences in conformations of chiral ligands can result in substantial changes in enantioselective reactions.

4.4.3 TADDOL-Based Complexes

A family of ligands that has frequently been employed in asymmetric catalysis with excellent results is the tartaric acid-based TADDOL ligands (**Figure 4.30**). Following the introduction of the parent TADDOL ligand, a large number of analogs with different aromatic substituents and ketal moieties were introduced.[71] TADDOL-based catalysts have found applications in a variety of Lewis acid catalyzed enantioselective reactions.[71] Upon deprotonation, the ligands bind well to early transition metals, forming strong M–O bonds[72] in the resulting TADDOLate complexes (**Figure 4.30**).

The conformational behavior in these ligands is similar to BINAP and chiraphos as outlined above. Based on the X-ray structural studies of unbound TADDOL ligands and of metal-bound TADDOLate complexes (**Figure 4.31**),[73,74] the features that make these ligands exceptional have been surmised. Upon coordination of TADDOL to metals, a trans-fused bicyclo[5.3.0]decane ring system results. The stereocenters of the dioxolane ring are too distant from the metal center in TADDOLate complexes to directly impact the enantioselectivity. Nevertheless, they impart a strong conformational preference on the adjacent metallacycle, positioning the diastereotopic aromatic groups such that they assume a pseudoequatorial/pseudoaxial arrangement. The pseudoaxial phenyl groups are positioned antiperiplanar to the neighboring dioxolane C–H bonds. In this fashion, the asymmetry of the stereogenic centers is relayed forward, toward the metal and the substrate-binding sites. There are some important differences, however, between the TADDOL and BINAP ligand systems. In the case of BINAP, the diastereotopic aryl groups are attached to the metal-bound phosphorus centers, while in TADDOL, these groups are bonded to the adjacent carbons. As a result, the aryl groups of the TADDOLate ligands are further removed from the metal, and the pseudoequatorial phenyl groups do not extend past the metal, as they do in BINAP complexes. Thus, it is the pseudoaxial aryl groups that are believed to be the dominant stereocontrolling element in TADDOL.[75]

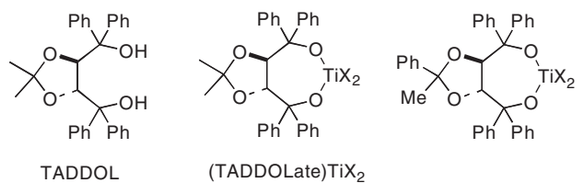

Figure 4.30. The parent (*R*,*R*)-TADDOL ligand and (TADDOLate)Ti complexes (X = halide or isopropoxide).

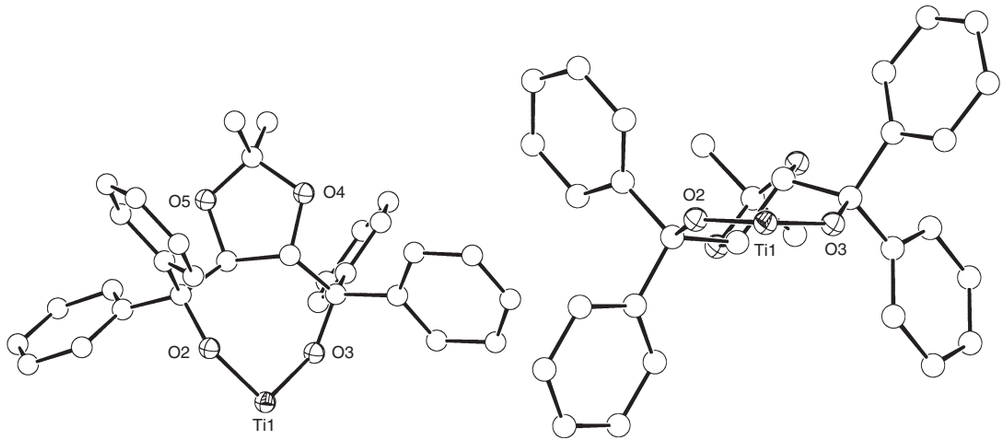

Figure 4.31. Partial structure of Ti(TADDOLate) moiety, illustrating the chiral environment about the ligand. The left view illustrates how the asymmetry in the metallacycle causes two rings to protrude forward and two to orient away from the metal center.

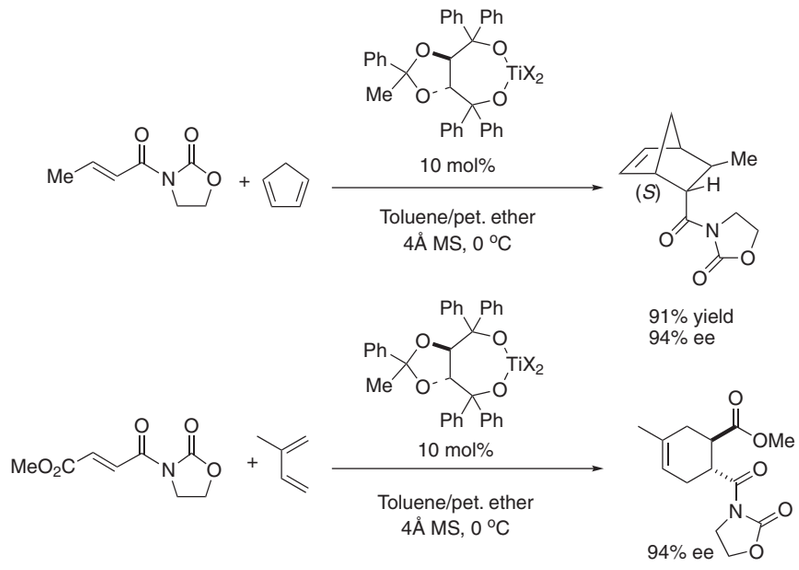

Figure 4.32. The (TADDOLate)Ti-catalyzed asymmetric Diels–Alder reactions.

Early examples of applications of TADDOL ligands in asymmetric catalysis were centered on the catalytic asymmetric addition of alkyl groups to aldehydes[71,76–78] and the asymmetric Diels–Alder reaction (**Figure 4.32**),[79] both using (TADDOLate)Ti-based complexes as the Lewis acids. The rapid exchange of alkoxide ligands and the notorious propensity of early metal alkoxides to aggregate through the formation of bridging alkoxides complicate studies of alkoxide-based catalysts.[72]

The story of the (TADDOLate)Ti-catalyzed Diels–Alder reaction[79] nicely illustrates a number of important points about the challenges of elucidating details of reaction

mechanisms and the transmission of asymmetry. Although the mechanism of this Lewis acid catalyzed process has been extensively investigated, some controversy remains about the geometry of the active substrate–catalyst adduct. In the reaction of the *N*-acyloxazolidinone with cyclopentadiene in the presence of (*R,R*-TADDOLate)$TiCl_2$, the expected *endo* adduct predominates with the (*S*)-configuration (**Figure 4.32**).[79] In this process, the dienophile is believed be to activated by chelation to titanium, giving rise to an octahedral substrate–catalyst adduct. In support of this binding mode, an X-ray crystallographic study of a substrate–catalyst adduct showed the substrate chelating to titanium. In the structure, the oxygens of the TADDOLate ligand and the coordinated substrate were located in the equatorial plane and the mutually trans chlorides were axial (**Figure 4.33**).[74] It was proposed that this adduct was the reactive intermediate that led directly to product on reaction with the diene.[74,80,81] Because the reactive C–C double bond of the dienophile is distant from the chiral environment of the TADDOLate ligand in this complex, it was unclear how the chiral ligand could bias the facial selectivity in the Diels–Alder cycloaddition. Furthermore, in the geometry of the substrate adduct in the crystal structure, the carbonyl oxygens of the dieneophile are each trans to the basic, electron-donating alkoxides of the TADDOLate ligand. This geometrical arrangement results in a low degree of activation of the substrate. Stronger activation would be expected if the carbonyl oxygen adjacent to the reactive double bond were trans to chloride.

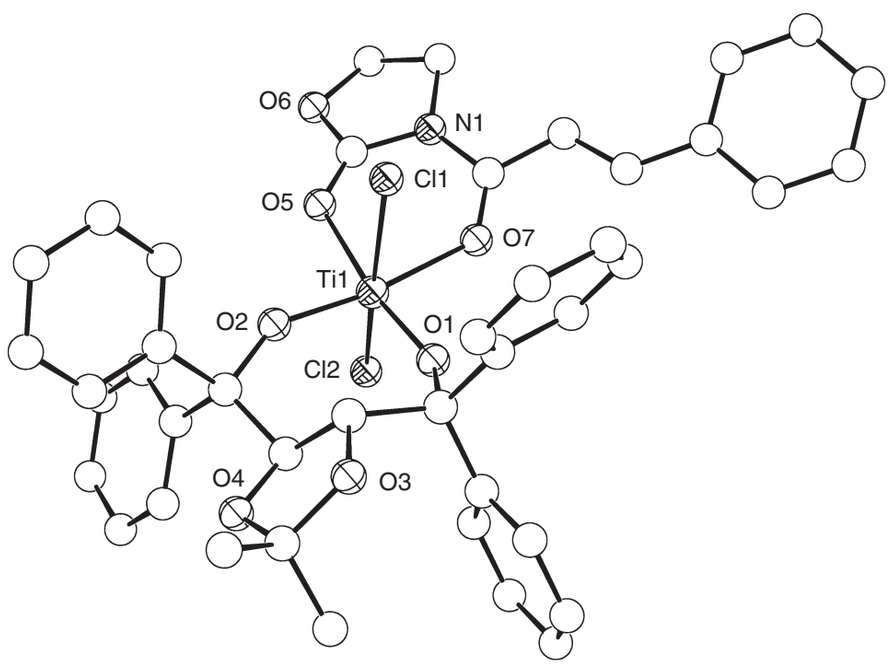

Figure 4.33. Structure of the (TADDOLate)$TiCl_2$ bound to the substrate.

Skepticism about the intermediacy of this adduct inspired further investigations into the solution behavior of the catalyst–substrate adduct in this reaction.[82,83] High-level quantum-chemical calculations were also employed to probe the degree of activation of the substrate with different arrangements of the ligands on the octahedral titanium center.[84] Analysis of the coordination modes of the substrate to the titanium center indicates that there are five possible geometries for this adduct, as illustrated in **Figure 4.34**. The bold vertical ligands in these structures represent the axial phenyl groups of the TADDOLate ligand. In isomer **A**, all of the oxygens lie in the equatorial plane. Diastereomers **B** and **C** have the carbonyl oxygen adjacent to the double bond trans to chloride while in **D** and **E** it is trans to a TADDOLate oxygen. In-depth NMR studies of (TADDOLate)$TiCl_2$ and the substrate indicted that only three of the five possible diastereomers were present in solution in a ratio of 70:24:6.[82] The major diastereomer in solution, **A** (**Figure 4.34**), was that observed in the crystal structure and calculated to be the most stable.[82,84] By positioning the TADDOLate ligand and the substrate in the equatorial plane, nonbonded interactions are minimized.

Experimental evidence into the precise geometry of the two less-abundant substrate–catalyst adducts was inconclusive. Perhaps more important than the geometries of the ground-state structure of these adducts is the degree of activation of the

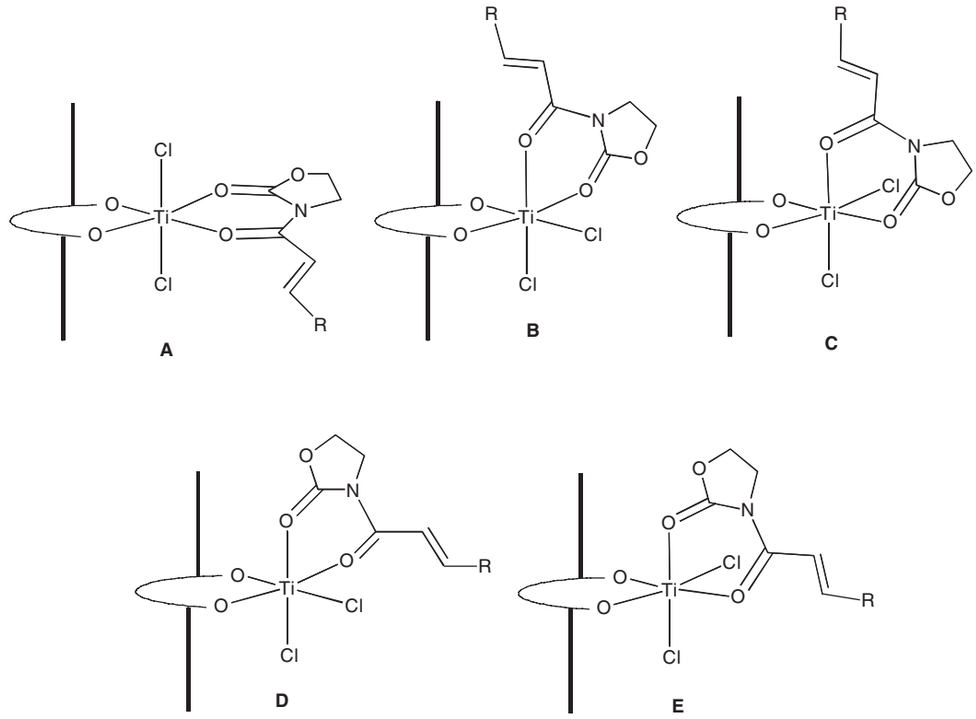

Figure 4.34. Five possible binding modes of the *N*-acyloxazolidinone to [(*R*,*R*)-TADDOLate]$TiCl_2$. The bold lines represent the pseudoaxial aryl groups of the TADDOLate ligand.

substrate by the titanium in geometries **A**–**E** in **Figure 4.34**, and hence their relative reactivity. High-level calculations on model systems predict that the bound substrate exhibits the greatest degree of activation in geometries **B** and **C**, because the carbonyl flanking the olefin is trans to the weakly donating chloride. The substrate in complexes **D** and **E** is predicted to be less reactive than in **B** and **C**, but more reactive than **A**.[84] Thus, although **A** is the most-stable diastereomer, as reflected in the high solution concentration and in the theoretical studies, it is believed to be the least reactive.

A plausible scenario for the reaction would involve reversible binding of the substrate to the titanium center. It has been found that exchange between bound and free substrate with (TADDOLate)$TiCl_2$ has a low barrier (15 kcal/mol) and proceeds via a dissociative pathway. This exchange is much faster than the cycloaddition, which is the stereoselectivity- and rate-determining step.[82] Based on the data outlined above, it has been proposed that the reaction falls under Curtin–Hammett conditions (see Section 2.5).[85] The reaction is funneled through a less-stable substrate–catalyst adduct, because of the greater reactivity of this intermediate and the fast equilibration of the diastereomeric substrate adducts.

In the substrate adducts **B** and **C** in **Figure 4.34**, the *Si* face is shielded by the pseudoaxial TADDOLate aryl group and the attack of the diene takes place from the *Re* face, as shown in **Figure 4.35**

This example illustrates several important points concerning the study of catalytic asymmetric reactions, including: 1) the way in which different arrangements of the ligands on the metal generate diastereomeric complexes that are chiral at the metal, 2) how different catalyst–substrate geometries exhibit unequal reactivities, and 3) how reactivity can be controlled by the Curtin–Hammett principle. It also demonstrates the application of a variety of experimental and computational tools to gain insight into various aspects of a reaction mechanism.

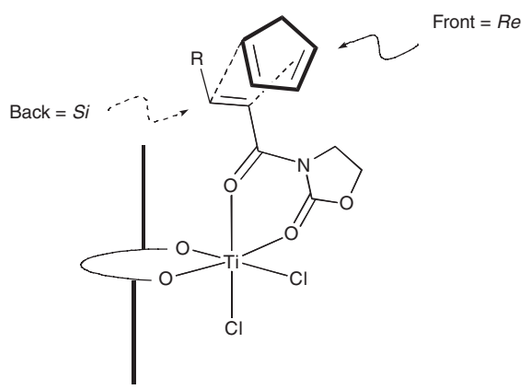

Figure 4.35. A possible transition state for the asymmetric Diels–Alder reaction where attack of the cyclopentadiene takes place on the α-carbon *Re* face of the dienophile, along the Ti–Cl axis.

4.5 Environments from Ligands That Form Diastereotopic Complexes

One of the challenges in the synthesis of chiral ligands is often the resolution of the components from which the ligand is assembled. It is frequently the case that resolutions of enantiomers is the most time-consuming step in the iterative cycle of catalyst screening, which involves the synthesis of new ligands, the preparation of catalysts, and the screening and evaluation of new catalysts. Therefore, if ligands can be designed such that a single stereocenter in the unbound ligand controls the generation of subsequent ligand stereocenters on binding to the metal, the number of stereocenters in the ligand–metal adduct can be increased, without additional resolutions.[86] Examples of this include selective coordination of diastereotopic lone pairs of the ligand to the metal, coordination of diastereotopic groups, and binding of the ligand in a diastereoselective fashion, such that the metal center becomes chiral. Furthermore, as outlined below, this interaction can serve to reduce the degrees of rotational freedom within the metal–ligand scaffold, thus extending and rigidifying the asymmetric environment of the catalyst.

4.5.1 Coordination of Diastereotopic Lone Pairs

The development of new enantioselective catalysts is, in part, dependent on the discovery and identification of innovative methods to transfer chirality from the catalyst to the substrate. A powerful method for catalyst development that has rarely been employed is diastereoselective binding of ligands to metals. In the process of binding the ligand to the metal, new stereogenic centers are formed either on the ligand or at the metal center. The diastereoselective coordination of an sp^3 hybridized lone pair on nitrogen or sulfur, for example, can increase the number of stereogenic centers upon coordination of the ligand.

Chiral diamines have been used in combination with zinc as catalysts for the asymmetric hydrosilylation of ketones with polymethylhydrosiloxane, $[–SiMe(H)O–]_n$. The precatalysts for this reaction were readily formed on combining diamines and dimethylzinc (**Figure 4.36**). In this reaction, the catalyst, which is proposed to be (diamine)ZnH_2, delivers hydride to the carbonyl carbon, resulting in a zinc alkoxide. The alkoxide reacts with the Si–H bonds of the polymer to generate a silyl ether, which undergoes hydrolysis on isolation to form the alcohol.[87]

When the reduction of acetophenone was performed using catalyst derived from diamines **A–C** (**Table 4.1**) and dimethylzinc, the (*R*)-alcohol product was observed.[88] Coordination of **A** to dimethylzinc results in formation of a five-membered metallacycle with fewer degrees of freedom than the six- or seven-membered metallacycles formed from **B** and **C**. When the short-chain ligand *N*,*N*′-ethylenebis(1-phenylethylamine) (**A**) was bound to dimethylzinc, the resulting complex showed

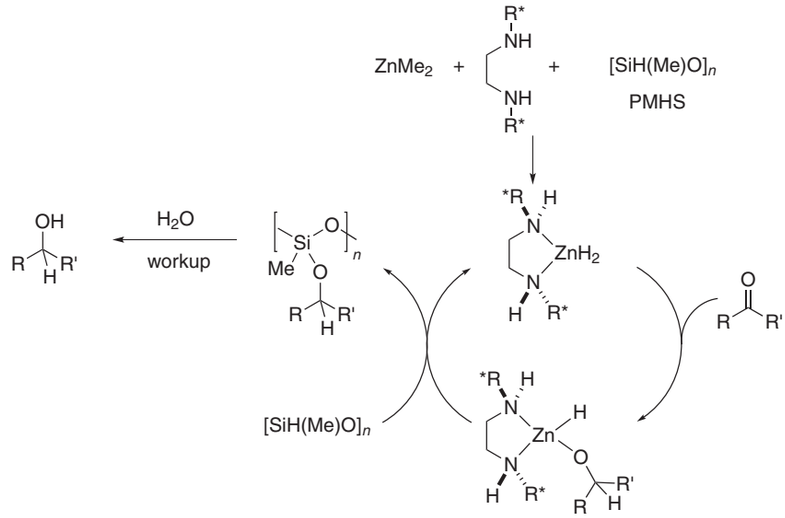

Figure 4.36. Proposed catalytic cycle in the zinc-diamine-catalyzed asymmetric reduction of ketones.

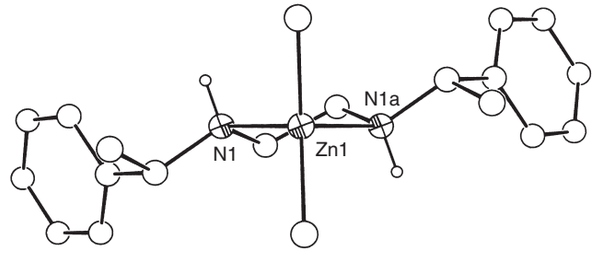

Figure 4.37. Structure of diamine **A** (see Table 4.1) coordinated to $ZnMe_2$, illustrating the configurations of the stereogenic nitrogen centers.

that stereochemical information in the chiral *N*-phenylethyl groups was effectively relayed to the nitrogen centers, which are rendered configurationally stable upon coordination. The *X*-ray crystal structure of this complex is illustrated in **Figure 4.37**, where the configuration of the nitrogens are *S*.[87] The stereogenic nitrogen centers are held in close proximity to the zinc, and have a significant impact on the enantioselectivity of the catalyst (79% enantioselectivity, **Table 4.1**). Increasing the tether length of the diamine backbone results in poor control of the configuration of the coordinating nitrogens, giving rise to diastereomeric zinc complexes. The mixture of diastereomers exhibits low levels of enantioselectivity in the asymmetric reaction (< 17% ee). Interestingly, the dimethylzinc complex of chiral diimine **D** was also shown to catalyze the reaction, but it gave the reduced product with the *opposite absolute configuration* in modest enantioselectivity (48% ee, **Table 4.1**). In this case, the nitrogen atoms in diimine **D** are sp^2 hybridized and the side chains are the only groups responsible for controlling the transfer of asymmetry in the reaction.

Table 4.1. Enantioselective reduction of ketones by polymethylhydrosiloxane in the presence of chiral zinc catalysts

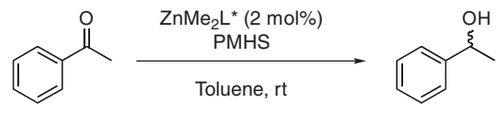

L*		Yield (%)	ee % (configuration)
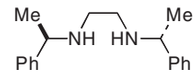	**A**	100	75 (*R*)
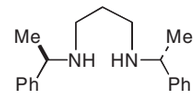	**B**	100	5 (*R*)
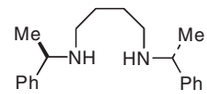	**C**	100	17 (*R*)
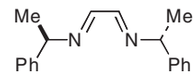	**D**	98	48 (*S*)

4.5.2 Binding of Diastereotopic Groups

Coordination of a diastereotopic atom to a coordinatively unsaturated metal can be important in enantioselective catalysis with many ligands. For example, bis(sulfonamide)-based catalysts can be highly active and enantioselective in a number of reactions, including the asymmetric alkylation of aldehydes (**Equation 4.5**).[89,90] This reaction allows preparation of functionalized secondary alcohols with excellent levels of enantioselectivity.[91]

Equation 4.5

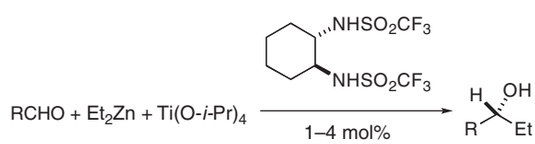

R	ee % (yield %)
Ph	98 (99)
PhCH=CH	85 (99)
$PhCH_2CH_2$	99 (92)
n-C_5H_{11}	78 (99)

Titanium complexes of the bis(sulfonamide) ligands have been proposed to be the active species in this reaction.[89,90,92,93] X-ray structure studies show long dative bond-

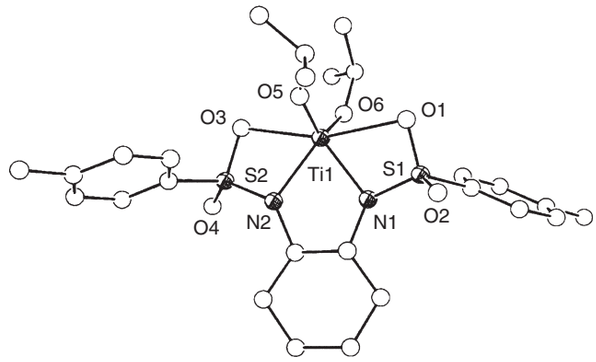

Figure 4.38. Illustration of the bonding in bis(sulfonamido)Ti(O *i*-Pr)$_2$ based on the crystal structure. The dative Ti–O(sulfonyl) bond distances are between 2.2 and 2.4 Å, compared to the covalent Ti–O(alkoxide) distances, which are 1.7–1.8 Å.

ing interactions between one of the diastereotopic oxygen atoms on each sulfonamide group and titanium.[93] This Ti–O(sulfonyl) interaction causes the sulfur atoms to be stereogenic and presumably rigidifies the C_2-symmetric ligand scaffold, as seen in **Figure 4.38**. In a sense, coordination of one of the diastereotopic sulfonyl oxygens to titanium extends the chiral environment of the ligand.[89,93–97]

Bis(sulfonamide) ligands are also important catalyst components in other reactions, including the asymmetric amination of *N*-acyloxazolidinones with magnesium,[98] the asymmetric cyclopropanation of allylic alcohols with zinc,[99–102] and the asymmetric Diels–Alder reaction with aluminum.[103] Magnesium bis(sulfonamido) complexes are Lewis acidic and presumably also coordinate the sulfonyl oxygens. Evidence for such interactions is found in related systems.[104] It is unlikely, however, that aluminum[103] and especially zinc[105] complexes of the bis(sulfonamide) ligands will bind the sulfonyl oxygens. In these systems, conformational gearing of the sulfonyl group with the chiral ligand backbone may extend the asymmetric environment, causing the high levels of enantioselectivity observed with these catalysts.

4.6 Electronic Asymmetry of Coordination Sites

Another example of a family of ligands that form an additional stereocenter upon coordination is the phosphorus-sulfur-based ligands in **Figure 4.39**. These ligands have been successfully employed in the asymmetric allylation with palladium[106,107] and the asymmetric hydrogenation (**Equation 4.6**) and hydrosilylation reactions with rhodium.[108]

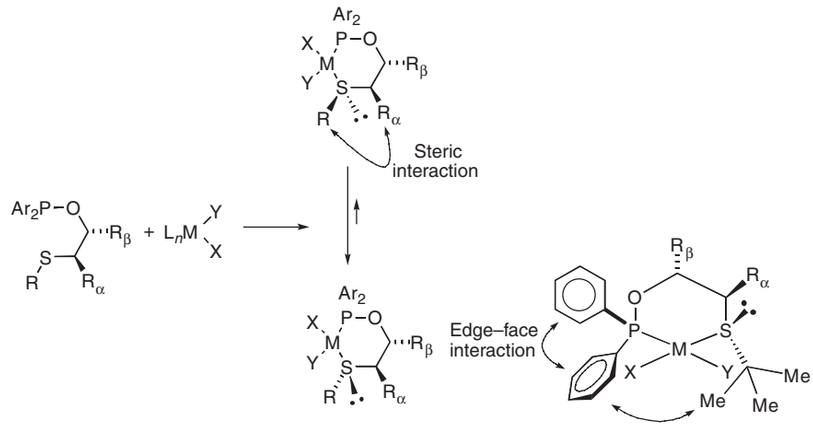

Figure 4.39. Binding of the P-S-ligand to metals forms two diastereomers that can interconvert by sulfur inversion or detachment of sulfur and recoordination.

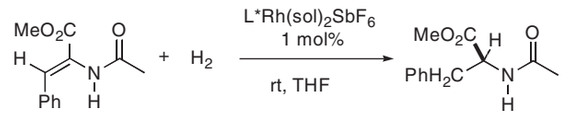

Equation 4.6

L*

R	ee (%)
Ph	95
3,5-C_6H_3-Me_2	97
CH_2Ph	90
Cy	NR
t-Bu	68

Metals bind to these ligands in a bidentate fashion, coordinating phosphorus and one of the diastereotopic lone pairs on sulfur (**Figure 4.39**). The resultant diastereomers (with the *S*-R oriented up and *S*-R oriented down) can readily interconvert by inversion of the coordinated sulfur lone pair, which has a low energy barrier, or detachment of the sulfur and re-coordination of the other lone pair. The degree of steric interaction between R_α and the sulfur-substituent R controls the extent to which the metal preferentially binds one of the diastereotopic lone pairs over the other and, therefore, the orientation of the *S*-R. The direct attachment of the stereogenic sulfur center to the metal, and its proximity to the substrate-binding site, make control of the orientation of the *S*-R substituent crucial to the effective stereochemical communication between the catalyst and the substrate. It has been found that the sulfur substituent is disposed in a pseudoaxial position to avoid nonbonded interactions with the R_α substituent, although electronic effects cannot be ruled out.[108,109] For bulky sulfur substituents, such as *t*-Bu, this group then influences the orientation of the *P*-phenyl groups. To minimize interactions between the sulfur substituent and the neighboring *P*-phenyl, the cis *P*-phenyl adopts an edge-on conformation, causing the remaining *P*-phenyl group to adopt a face-on orientation.[109,110]

An additional feature of mixed heteroatom donor ligands, such as the P-S-ligand in **Figure 4.39**, is that they electronically differentiate their respective trans binding

sites. In this case, the phosphorus ligand is a stronger trans donor than sulfur, making ligand Y more labile than ligand X (**Figure 4.39**). The trans effect will impact how chelating substrates bind, with the weakest trans donor opposite the strongest.

Using this P-S-ligand system, a detailed study of the mechanism of the asymmetric hydrogenation was undertaken. The catalyst–substrate adduct was independently synthesized and characterized by X-ray crystallography. A drawing of the structure is illustrated in **Figure 4.40**. By ^{1}H and ^{31}P NMR spectroscopy only a single diastereomer was observed in solution out of the four possibilities.

Beginning with the diastereomer in the crystal structure (**A**, **Figure 4.41**), the unobserved diastereomers can be drawn by reversing the positions of the carbonyl and double bond (**B**) and coordination of the opposite face of the olefin (**C** and **D**).

The observed diastereomer is favored by a combination of the steric constraints of the bound ligand and the electronic factors caused by the unequal trans influence of the phosphorus and sulfur donors. The bulky sulfur substituent and the neighboring edge-on aryl group block the lower two quadrants around the metal center, leaving the upper quadrants sterically unencumbered (**Figure 4.42**). The left half and right half of the diagram are electronically inequivalent by virtue of the differing trans influence of the phosphorus and sulfur, which favor binding the weaker trans donor of the substrate opposite the strongly donating phosphorus center. The trans influence is represented by the checkered regions of the quadrant diagram. In the substrate, the C–C double bond has a stronger trans influence than the carbonyl lone pair and

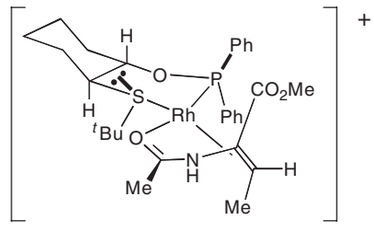

Figure 4.40. Drawing of the intermediate formed on coordination of the substrate to rhodium (based on the an X-ray crystal structure of this complex).

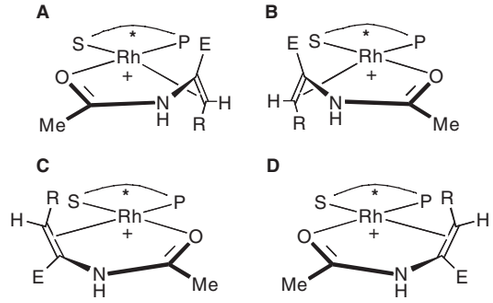

Figure 4.41. Possible diastereomers of the substrate coordinated to (P-S)Rh^{+} moiety (**Figure 4.40**). Diastereomer **A** is predicted to be the most stable and is observed in the crystal structure.

will prefer to bind opposite the weaker sulfur donor (**Figure 4.42**) With this system, the stereochemistry of the catalyst–substrate complex correlates with the observed stereochemistry of the reduced product. As discussed in Section 2.5, this is not always the case in asymmetric hydrogenation reactions.

Like the (BINAP)Ru-catalyzed hydrogenation of β-keto esters, the mechanism is proposed to involve initial loss of solvent ligands, chelation of the substrate as described above, followed by oxidative addition of H_2 (**Figure 4.43**). Note that in the oxidative-addition product, the ligand with the strongest trans influence (phosphorus and the hydrides) are positioned trans to the three weakest donors. In intermediate **B**, the olefin is correctly aligned for the migratory-insertion step, which establishes the product stereochemistry. The resultant alkyl hydride (**C**) undergoes reductive

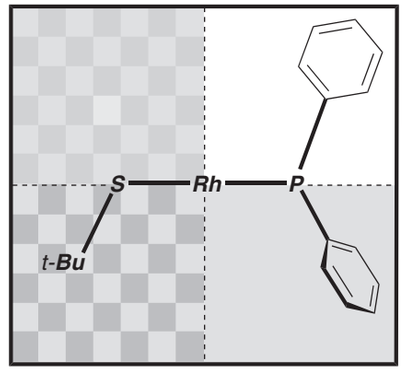

Figure 4.42. Model for the occupied space and electronic effects in the rhodium complex of a P-S-chelating ligand. The darker areas are occupied by the ligand. The checkered regions lines indicate the binding site trans to the strong trans influence of the phosphine ligand.

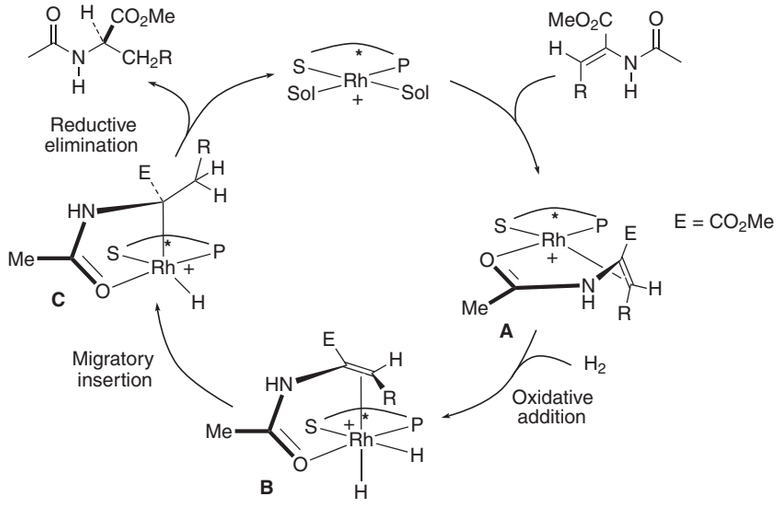

Figure 4.43. Proposed mechanism of the (P-S)Rh^+-catalyzed hydrogenation of α-acylaminoacrylates.

elimination to form the stereocenter. Subsequent dissociation of the product, which does not bind well to the rhodium, then occurs.

To recap, the transmission of asymmetry in this system is dominated by the orientation of the *S*-R substituent, which is, in turn, dictated by the adjacent stereocenter. The orientation of the *S*-R group further biases the neighboring cis *P*-phenyl substituent. To minimize the transannular interaction, the cis *P*-phenyl orients an edge toward the substrate binding site, sterically blocking this quadrant. Additionally, the trans influence dictates diastereoselectivity in substrate binding and the oxidative addition of dihydrogen.

4.7 Steric Bias of Configurationally Dynamic Ligand Stereocenters

4.7.1 Ligands with Chiral Relay Groups Not Directly Connected to the Metal

A clever catalyst design based on stereochemically dynamic functional groups employs the dihydropyrazole moiety, where a fixed stereocenter controls the configuration of two fluxional nitrogen stereocenters (**Figure 4.44**).[111] The stereogenic nitrogen bearing the CH_2R substituent is remote, but exhibits a marked impact on the catalyst enantioselectivity. The stereochemistry of the *N*-methyl group of the amino alcohol is *anti* to the adjacent stereocenter to avoid an unfavorable eclipsing interaction. Data from reactivity studies suggest that the ligand is bound in a tridentate fashion and likely adopts a meridinal geometry as shown in **Figure 4.44**.

Application of these complexes in the asymmetric Diels–Alder reaction was explored to evaluate the influence of the substituent R on the enantioselectivity of the catalyst (**Figure 4.45**). The results of this study suggest that the size of the R group plays a crucial role in the enantioselectivity of the catalyst (**Figure 4.45**). As the size

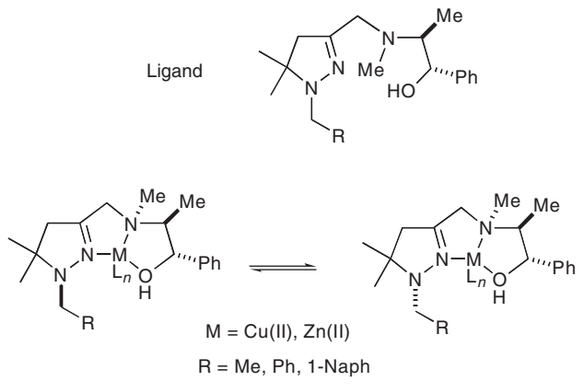

Figure 4.44. A ligand with a chiral relay is shown. Coordination to metals establishes two additional stereocenters. Interconversion of two possible diastereomeric complexes through nitrogen inversion is shown.

of the remote substituent R is increased from methyl to 1-naphthyl, the enantioselectivity of the product rises from 50% to > 90% ee for both diastereomeric products. From these data, it is clear that the size of the stereochemically labile NCH_2R group is the primary determinant of the degree of facial selectivity.

A proposed model to rationalize the role of the stereolabile NCH_2R group and the enantioselectivity is illustrated in **Figure 4.46**. The dieneophile, shown in bold, is bound in a bidentate fashion. A reasonable assumption is that the *N*-acyl moiety of the substrate will bind in the axial position on the face opposite the pseudoequatorial phenyl. As a result, the CH_2R group will likely be directed downward to reduce nonbonded interactions between the relay substituent and the substrate. To minimize steric strain between one of the geminal dimethyl groups and the chiral relay, the CH_2R group is expected to be oriented toward the bound substrate (**Figure 4.46**). In this conformation the naphthyl group shields the *Re* face of the substrate, consistent with the observed sense of stereoselection. One advantage of the catalyst possessing stereochemically dynamic groups is that several ligands can often be constructed

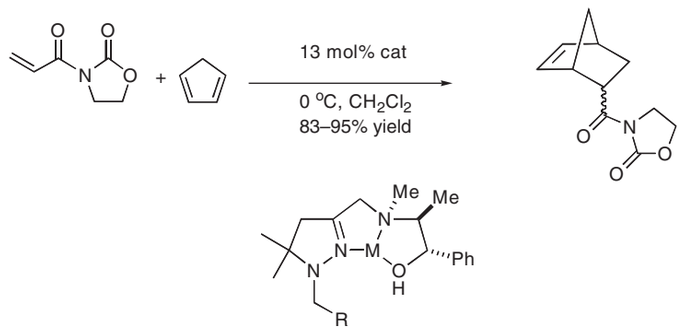

M = $Cu(OTf)_2$			M = $Zn(OTf)_2$		
R	*endo*/*exo*	ee *endo* [*exo*]	R	*endo*/*exo*	ee *endo* [*exo*]
Me	4.6	59 [60]	Me	3.9	54 [41]
Ph	3.2	82 [92]	Ph	3.4	89 [87]
1-Naph	2.4	92 [97]	1-Naph	3.8	96 [95]

Figure 4.45. Asymmetric Diels–Alder reaction using stereochemically dynamic ligands.

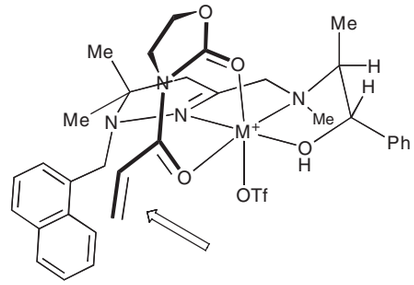

Figure 4.46. Proposed transition state for the asymmetric Diels–Alder reaction. The dienophile is shown in bold, and one of the triflate anions is proposed to occupy an axial position.

from a single resolved starting material, thus permitting rapid assembly of a family of ligands.[111]

4.7.2 Catalysts That Are Chiral at the Metal Center

One of the guiding principles in the design of asymmetric catalysts is that the metal is in a chiral environment. As we have seen, this can be accomplished in several ways, including projection of stereochemical information from remote centers toward the metal by the conformational preferences of the ligand–metal adduct or, at the other extreme, positioning the stereocenters in close proximity to the metal center. This latter strategy can be taken one step further by designing catalysts such that the metal center is a stereogenic center.[112,113] The synthesis of compounds where the sole chiral element is the metal center is very difficult, and is an area that remains to be developed (see Section A.1.1.b). Less difficult, but still tricky, is the synthesis of catalysts in which a chiral ligand binds to the metal center, causing the metal to become a stereocenter. The challenge is maintaining the stereochemical integrity of the catalyst over the course of the reaction, because the coordination number of the metal inevitably changes, providing an opportunity for the stereochemistry of the metal to scramble. As we will see in Chapter 6, use of diastereomeric catalysts can complicate optimization of asymmetric processes. However, if the energy difference between the diastereomeric catalysts is sufficiently large, thermodynamics may insure that only a single diastereomer is generated.

Reaction of dimeric $[(\eta^6\text{-arene})MCl_2]_2$ (M = Ru, Os) with the P/O ligand BINPO and $NaSbF_6$ resulted in formation of $[(\eta^6\text{-arene})MCl(BINAPO)][SbF_6]$, an 18-electron, coordinatively saturated complex (**Figure 4.47**). To facilitate access to an open

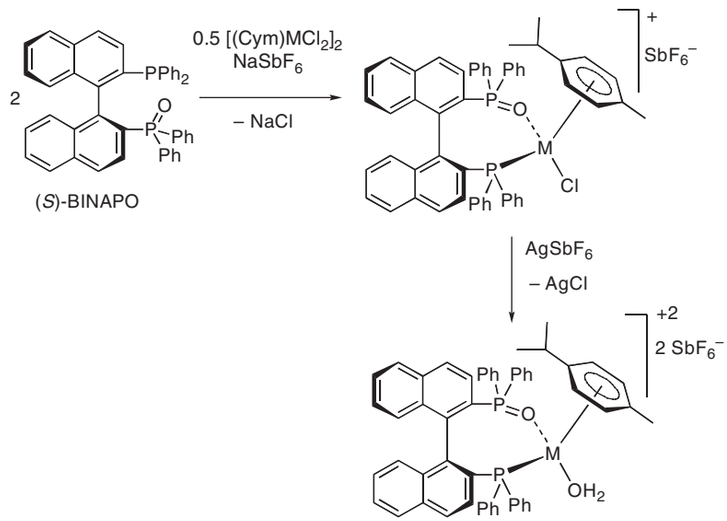

Figure 4.47. The synthesis of diastereomeric BINAPO complexes of ruthenium and osmium. The metal can be considered pseudotetrahedral.

coordination site, the remaining chloride was removed by treatment with $AgSbF_6$ to give the dicationic aqua complex $[(\eta^6\text{-arene})M(OH_2)(BINAPO)][SbF_6]_2$. Analysis of the ^{31}P and ^1H NMR spectra of the ruthenium and osmium complexes indicated formation of a single diastereomer in each case.

These compounds were then used in the Lewis acid catalyzed asymmetric Diels–Alder reaction of cyclopentadiene with methacrolein, a monodentate dienophile (**Figure 4.48**). The enantioselectivities with both the osmium and ruthenium systems were excellent.[114,115]

The X-ray crystal structure of $[(\eta^6\text{-arene})OsCl(BINAPO)]^+$ is illustrated in **Figure 4.49**. Based on this structure, a catalyst–substrate adduct has been proposed, and a partial structure showing the arrangements of ligands around the metal center is illustrated in **Figure 4.50**. A transition state to explain the sense of enantioselectivity is illustrated on the bottom of **Figure 4.50**.

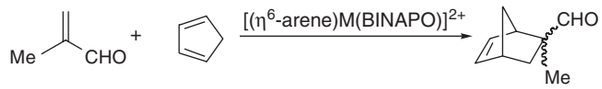

Catalyst (mol%)	Configuration	*exo*:*endo* ratio	ee (%)
Os (4)	R_{Os},S_{BINPO}	98:2	93 (*S*)
Ru (10)	R_{Ru},S_{BINPO}	96:4	99 (*S*)

Figure 4.48. Asymmetric Diels–Alder reactions catalyzed by osmium and ruthenium complexes of BINAPO.

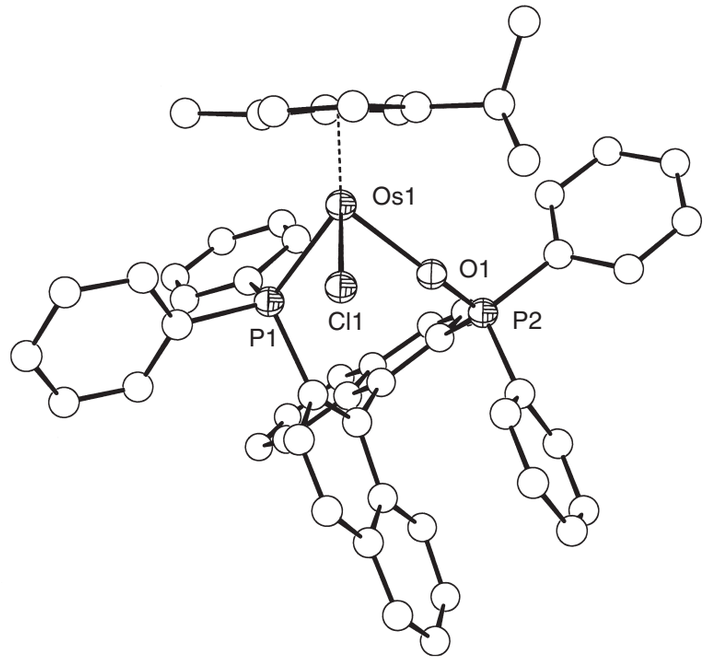

Figure 4.49. Structure of $[(\eta^6\text{-arene})OsCl(BINAPO)]^+$. The P–Os–O bond angle is 161.5°.

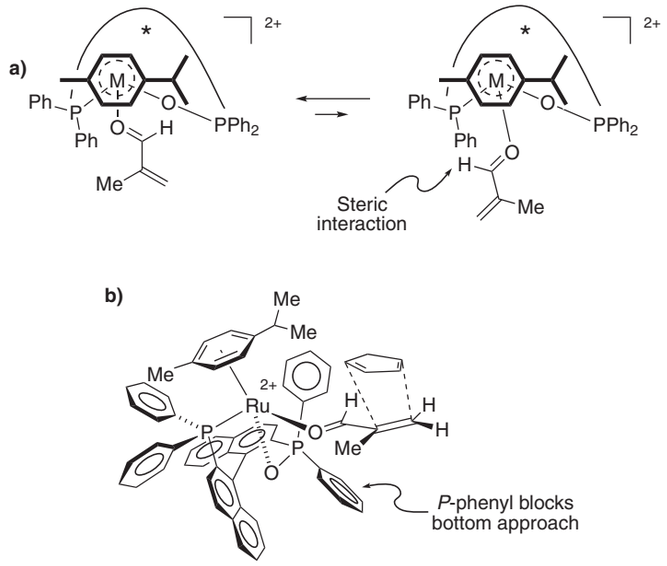

Figure 4.50. a) View from above the η^6-arene of the dienophile coordination (recall that the P–Os–O bond angle of BINAPO is 161.5° in Figure 4.49). Two proposed aldehyde conformations are shown. b) Proposed transition state for the Diels–Alder reaction.

4.7.3 Ligands That Can Adopt Atropisomeric Conformations

Ligands with axial chirality, such as BINAP and BINOL, have been shown to form highly enantioselective catalysts with a variety of metals in many asymmetric transformations. Not only are these ligands extremely adept at inducing asymmetry in prochiral substrates, they also efficiently transfer asymmetry to stereochemically flexible groups within a ligand.[86,116–118] The preparation of substituted derivatives of these popular ligands in enantiomerically pure form can be a laborious process, inspiring investigators to circumvent resolution of atropisomeric moieties, when possible. Below are some methods that have been successfully used in this context.

4.7.3.a Axial Chirality Induced in Backbone Biphenyl-Based Ligands

The binaphthyl ligand in **Figure 4.51** possesses central chirality and a fixed chiral axis,[119] whereas the biphenyl derivative has a conformationally mobile axis.[120] ^{1}H NMR spectra of the biphenyl ligand exhibit two diastereomeric complexes in approximately a 1:1 ratio that interconvert via rotation about the biphenyl axis.[120] Addition of $[(\eta^3\text{-1,3-diphenylallyl})PdCl]_2$ (0.5 equivalent) could give up to four diastereomers—namely, two diastereomeric configurations of the chiral axis and two orientations of the 1,3-diphenylallyl ligand (**Figure 4.52**). Only two diastereomers were observed—one W- and one M-type allyl, both with the (*S*)-configuration of the chiral axis. The configuration of the chiral axis was assigned by observation of a negative Cotton effect at 250 nm in the CD spectrum.[121,122] Thus, the central chirality

causes the diastereomeric ligand conformations to have significantly different energies once coordinated to the (η^3-1,3-Ph_2allyl)Pd moiety.

Comparison of the binaphthyl and biphenyl ligands in **Figure 4.51** was undertaken in the asymmetric allylation of 1,3-dipehnyl-2-propenyl acetate with dimethyl malonate (**Figure 4.53**) under conditions almost identical to those in **Figure 4.10**. Use of the binaphthyl ligand with the fixed (*S*)-chiral axis (R = *i*-Pr) gave 85% ee of the (*S*) product (**Figure 4.53**). The conformationally dynamic biphenyl ligand (R = *i*-Pr) exhibited very similar enantioselection [83% ee of the (*S*)-product], while the *t*-Bu derivative gave slightly higher enantioselectivity. Application of the diastereomeric binaphthyl ligand with the fixed (*R*)-chiral axis resulted in formation of the opposite enantiomer of the product with 90% ee. Several important conclusions can be drawn from these results. The advantage of the use of the dynamic biphenyl-derived ligand is that it gives slightly higher enantioselectivity than the more synthetically challeng-

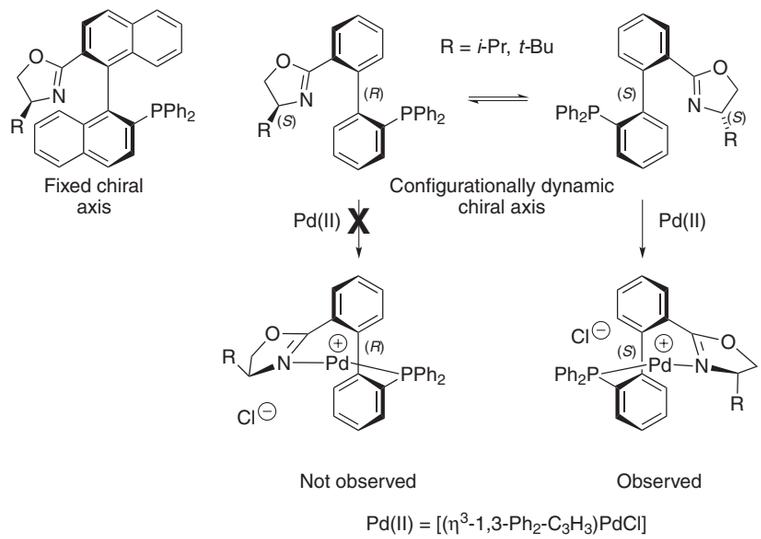

Figure 4.51. A binaphthyl ligand with central chirality and a fixed chiral axis (top left) and a biphenyl ligand with central chirality and a conformationally dynamic axis (top right). Reaction with [(η^3-1,3-Ph_2allyl)PdCl] affords the complex with the (*S*)-chiral axis (also see **Figure 4.52**). The allyl moiety is removed for clarity.

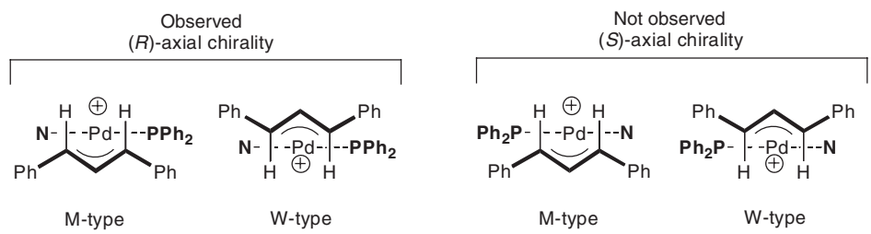

Figure 4.52. The four possible diastereomeric allyl complexes. The allyl can have the M- or W-type orientation with respect to the Ph_2P---N ligand plane. The biphenyl-derived ligand can have the (*S*)- or (*R*)-axial chirality.

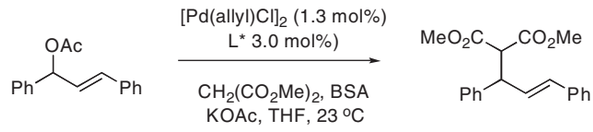

Entry	Ligand	R	Yield (%)	ee % (configuration)
1	(a*S,S*)-binaphthyl	*i*-Pr	93	85 (*S*)
2	(*S*)-biphenyl	*i*-Pr	95	83 (*S*)
3	(*S*)-biphenyl	*t-Bu*	97	88 (*S*)
4	(a*R,S*)-binaphthyl	*i*-Pr	93	90 (*R*)

Figure 4.53. Palladium-catalyzed allylic alkylation with ligands from **Figure 4.51**. In each case, the central chirality has the (*S*)-configuration (BSA = bissilylacetamide).

ing fixed binaphthyl ligand. The disadvantage of the dynamic chiral axis, however, is that only one of the diastereomeric combinations can be access [the (*S*)-central chirality induces only the (*S*)-axial chirality, **Figure 4.51**]. In this particular case, the ligand with (*S*)-central chirality and (*R*)-axial chirality (**Figure 4.51**) gave slightly higher enantioselectivity (90% ee, entry 4, **Figure 4.53**).

This approach has been applied successfully to other catalytic asymmetric reactions[123] and will likely attract more attention in an effort to streamline ligand syntheses.

4.7.3.b Axial Chirality Induced in Pendant Biphenyl-Based Ligands

Diphosphite ligands **A–D** (**Figure 4.54**) have been used in the rhodium-catalyzed reduction of dimethylitaconate to afford chiral diesters. The phosphite ligands employed are composed of two groups, a nonracemic sugar-based backbone linker and BINOL-, biphenol-, or 2-naphthol-derived pendent groups. BINOL-derived ligands $\mathbf{A}_S$ and $\mathbf{A}_R$ provide diastereomers that differ in the relative configurations of the backbone and the binaphthyl groups. Ligands **B** and **C** (**Figure 4.54**) contain conformationally flexible groups that can undergo atropisomerization. These groups relay the stereochemistry of the ligand backbone toward the metal center. This process has a low barrier, insuring rapid interconversion of the diastereomeric ligands and, therefore, catalysts.[124] Although three diastereomers of ligands **B** and **C** are possible, it is unlikely they will be present in equal amounts, because the stereochemistry of the biphenol moieties depends on their interaction with the chiral backbone. Ligand **D** contains 2-naphthoxy groups that cannot adopt atropisomeric conformations.

When (*S*)- or (*R*)-BINOL-based ligands ($\mathbf{A}_S$ and $\mathbf{A}_R$) were employed, the enantioselectivities were very high, but the sense of enantioselection was opposite (**Table 4.2**). Axial chirality of the pendent groups is dominant in determining the configuration of the product. The magnitude of the enantioselectivities from $\mathbf{A}_S$ and $\mathbf{A}_R$ is similar, suggesting that the chiral linker has almost no impact on the catalyst enantioselectivity.

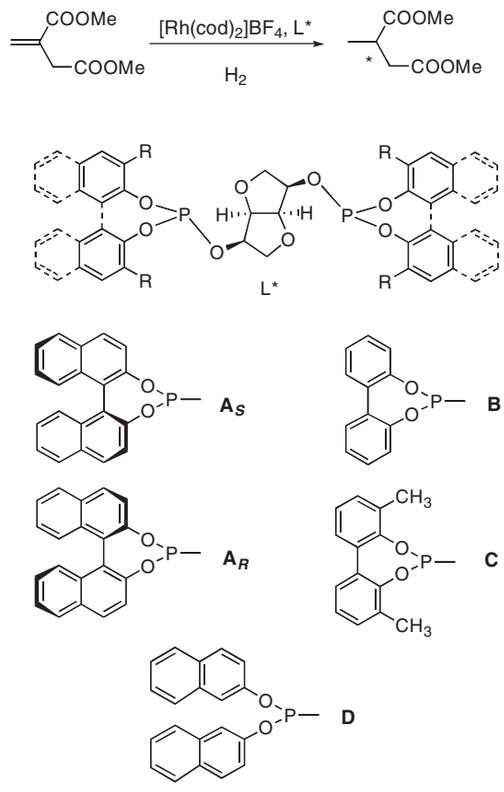

Figure 4.54. Asymmetric hydrogenation of dimethylitaconate with chiral diphosphite ligands.

Employing biphenol-based ligand **B**, which possesses the conformationally flexible pendent moieties, gave intermediate enantioselectivity (39%) favoring the (*S*) product. It is possible that this ligand gives rise to diastereomeric catalysts that operate simultaneously in the reduction reaction. Conclusions about the proportions of the diastereomeric catalyst based on the enantioselectivity, however, is not possible, because the catalysts are likely to have different relative rates.

The highest enantioselectivities (97% ee) were obtained with ligand **C** substituted with methyl groups at the 3- and 3′-postions. The enantioselectivity was slightly higher than with ligands $\mathbf{A}_S$ and $\mathbf{A}_R$, based on the stereochemically fixed BINOL (**Table 4.2**). Direct comparison between ligands **C**, $\mathbf{A}_S$, and $\mathbf{A}_R$ is complicated due to the absence of the 3,3′-substituents in $\mathbf{A}_S$ and $\mathbf{A}_R$. It is interesting to note that the order of activity of the catalysts parallels their enantioselectivity: $\mathbf{A}_S < \mathbf{A}_R < \mathbf{C}$. In the case of ligand **D**, which cannot adopt atropisomeric conformations, the product has low ee (21%).

The advantage of incorporating stereochemically dynamic groups into ligands allows one to create a ligand library based on a single chiral backbone. The drawback is that the optimal catalyst must be generated by screening a series of chiral ligands. As outlined in subsequent chapters, a more efficient method to develop asymmetric catalysts is based on the combination of chiral and achiral ligands.[125] In this fashion, a single chiral ligand can be used to generate a family of catalysts.[126]

Table 4.2. Enantioselectivities in the asymmetric hydrogenaiton of dimethylitaconate with catalysts based on ligands **A–D** (**Figure 4.54**).

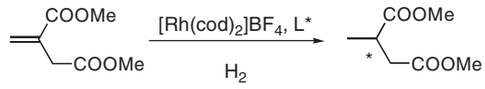

L*	Conversion at 20 h (%)	ee (%)
$\mathbf{A}_S$	> 99	88 (*S*)
$\mathbf{A}_R$	> 99	95 (*R*)
B	74	39 (*S*)
C	> 99	97 (*R*)
D	65	21 (*S*)

4.7.3.c Axial Chirality Induced in Atropisomeric Amides

Almost all of the atropisomeric ligands (i.e., ligands that are chiral by virtue of hindered rotation) are biaryls. Examples that we have seen are BINAP and BINOL. These ligands are stable to racemization under typical reaction conditions. The use of other types of atropisomeric ligands is uncommon, in part due to difficulties in the synthesis of such ligands. Nonetheless, once this obstacle is overcome, the use of other types of atropisomeric ligands will likely be more common. An interesting strategy that takes advantage of atropisomeric conformations has been employed in the asymmetric allylation with palladium. In this system, the central chirality of a fixed stereocenter biases the conformation of a stereochemically dynamic atropisomeric amide.[127,128]

As illustrated in **Figure 4.55**, use of the atropisomeric amide-based phosphine ligand in the palladium-catalyzed allylic alkylation with dimethyl malonate gave 85% ee. Although no structural information has been reported concerning the (π-allyl)Pd complex in the reaction, NMR data suggest the ligand is bidentate, coordinating to the palladium through the phosphorus and amide-carbonyl oxygen. In this adduct, the extant carbon stereochemistry will influence the disposition of the axial chirality of the amide, as well as the orientation of the two *P*-phenyl groups (see Section 4.3.2).

The central chirality of this ligand is sufficiently removed from the metal center that it is unlikely to be directly responsible for the excellent control of enantioselectivity in the allylation reaction. It is more plausible that the transmission of asymmetric induction is relayed through the axial conformation of the amide and the orientation of the diastereotopic *P*-phenyl groups.[110]

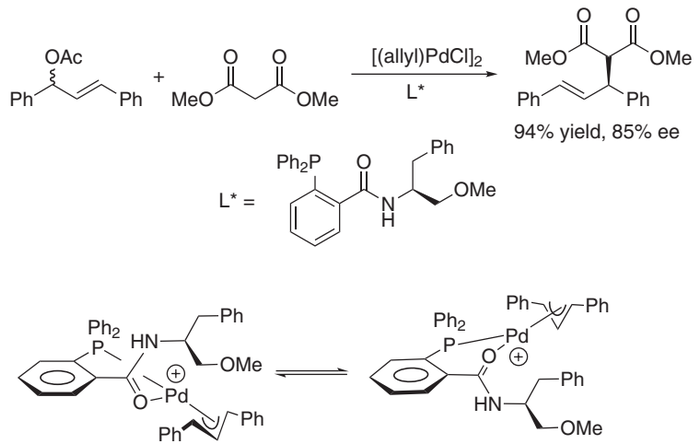

Figure 4.55. Asymmetric allylic alkylation using atropisomeric amides as chiral ligands (top) and the possible diastereomeric allyl intermediates (bottom).

4.8 Induced Asymmetry in the Substrate

4.8.1 Diastereomeric Complexes with Prochiral Substrates

A similar chelation of a sulfonyl oxygen to that in Section 4.5.2 was proposed based on density functional theory calculations in a study of the copper-catalyzed aziridination of alkenes using [*N*-(*p*-toluenesulfonyl)imino]phenyliodinane (PhI=NSO_2Tol) as the nitrene source (**Figure 4.56**).[129] In systems employing the bisoxazoline[13,130] and diimine[131,132] ligands, the reaction is believed to proceed through a Cu(I)/Cu(III) couple, and evidence for an intermediate copper nitrene has been presented.[129,132]

As illustrated in **Figure 4.57**, coordination of the sulfonyl oxygen gives rise to diastereomeric intermediates differing in the configuration at sulfur. The calculations suggest that the sulfonyl oxygen remains bound to copper during the formation of the N–C bonds.[129] Although the impact of the stereogenic sulfur center has not been in-

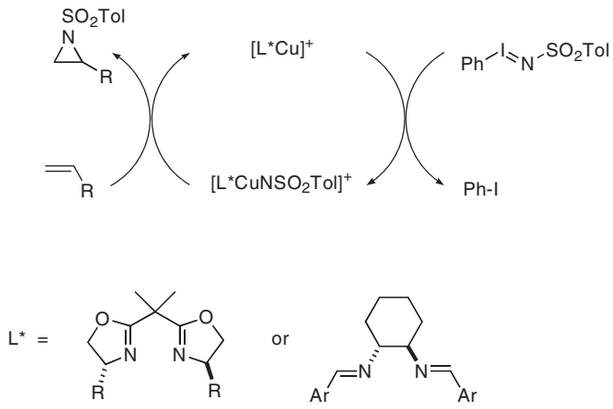

Figure 4.56. Catalytic aziridination of olefins with copper catalysts.

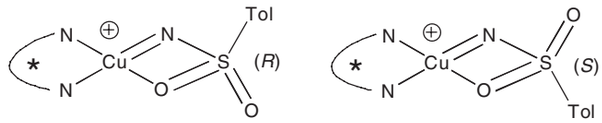

Figure 4.57. Diastereomers formed on coordination of the sulfonyl oxygen in the intermediate nitrene proposed for the aziridination of olefins.

vestigated, it is likely to be significant, based on its proximity to the reactive nitrogen of the nitrene.

4.8.2 Substrates with Chiral Relays

We have seen examples where the chiral metal–ligand adduct controls the attack of a reagent on a bound substrate, and examples in which the catalyst controls the binding of a substrate prochiral face in the enantioselectivity-determining step. A distinct and ingenious approach involves transmission of stereochemical information from a chiral catalyst to a stereolabile center in the substrate, termed a chiral relay, which then controls the stereochemistry of attack at that substrate by an external reagent.[133]

An example of a chiral relay built into the substrate is illustrated in **Figure 4.58**. In this approach, a rapidly racemizing amino group is incorporated into the substrate. The role of the asymmetric catalyst is to bind the substrate and temporarily transform the stereochemically labile nitrogen into a chiral auxiliary. In turn, this stereocenter directs the approach of the incoming reagent.

These substrates were used in asymmetric Diels–Alder reaction catalyzed by the now familiar bisoxazoline–copper(II) complexes. The substrates for this reaction are butenoylpyrazolidinones having different *N*-alkyl relays, R (**Figure 4.59**). Two routes to coordination and activation of the substrate can be envisioned. The bound substrate can undergo epimerization and equilibrate to the lower-energy diastereomer or

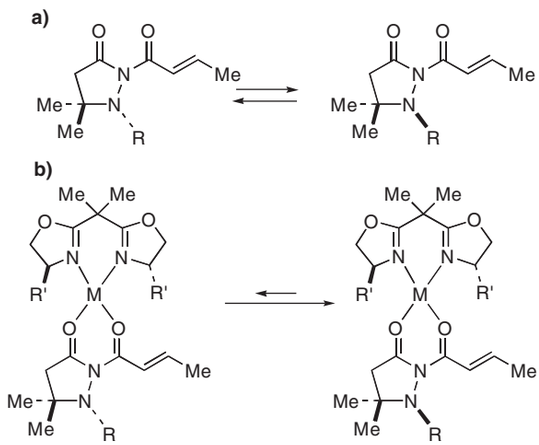

Figure 4.58. a) Nitrogen inversion racemizes the substrate. b) Diastereomeric substrate–catalyst adducts can epimerize through nitrogen inversion. These diastereomers may be very different in energy.

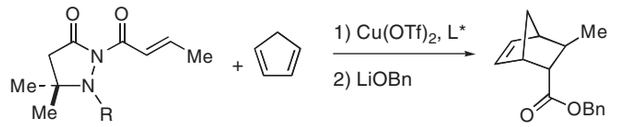

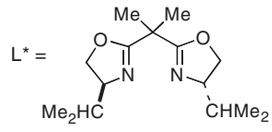

Substrates	ee (%)
R = H	08
R = Et	56
R = Bn	71
R = 2-CH_2-Naph	65
R = 1-CH_2-Naph	92

Figure 4.59. Impact of chiral relay groups, R, on the enantioselectivity of the asymmetric Diels–Alder reaction. The second step cleaves the relay portion of the substrate.

one enantiomer of the racemizing substrate can selectively bind to the chiral catalyst before activatation (**Figure 4.58**).

In this study, a comparison was made between the relay group on the substrate and the enantioselectivity (**Figure 4.59**). As progressively larger chiral relay groups were used, the enantioselectivity increased. The observed ee range (8–92%) clearly indicates that the enantioselectivity is highly dependent on the size of the chiral relay. Furthermore, the large variation in enantioselectivity suggests that the bisoxazoline ligand is not solely responsible for the enantioselectivity. It was also demonstrated that the enantioselectivities with the most efficient chiral relays were independent of the substituents on C_2-symmetric bisoxazoline ligands. This evidence also indicates that the chiral relay is responsible for control of the facial attack of the diene.[133,134] Although the concept of chiral relays should be applicable to other types of substrates, it is not limited to incorporation into the substrate (see Section 4.7.1).

Concluding Remarks

The basic concepts describing the transmission of asymmetry in chiral catalysts have been outlined in this chapter, with a focus on ligand classes most commonly encountered in asymmetric catalysis. This foundation will be expanded in Chapter 5, which describes nonclassical two-point catalyst-substrate interactions. Some of the systems presented in this chapter have been extensively researched and the proposed models advanced are widely accepted. Other examples have been more recently introduced, yet hold considerable potential for both expansion and applications.

Understanding the fundamental concepts outlined herein is necessary, although not sufficient in and of itself, to rationally design new enantioselective catalysts. It is also valuable to know the basic characteristics of the reaction of interest. For example, how do the ligand and substrate bind to the metal, what is the metal coordination number, and what is the metal geometry? While determination of these features may

appear trivial, it is not always the case. Furthermore, to increase the likelihood of success, a detailed knowledge of the reaction mechanism is helpful. Even after achieving the level of understanding outlined above, the design of asymmetric catalysts is challenging, because the energy differences between diastereomeric transition states are inherently small and currently beyond our ability to reliably predict or calculate. In the end, there is no substitute for the iterative cycle of catalyst optimization, consisting of catalyst design, screening, analysis of the results, and catalyst modification. This process can be dramatically streamlined, however, with knowledge of the reaction mechanism and the mode of transmission of asymmetry from the catalyst to the substrate. As is so often true in chemistry, the age-old saying that "luck (success) favors the prepared mind" holds true.

References

(1) Kagan, H. B.; Phat, D.-T. Asymmetric Catalytic Reduction with Transition Metal Complexes. I. Catalytic System of Rhodium(I) with (–)-2,3-O-Isopropylidene-2,3-dihydroxy-1,4-bis(diphenylphosphino)butane, a New Chiral Diphosphine. *J. Am. Chem. Soc.* **1972**, *94*, 6429–6433.

(2) Kagan, H. B. In *Asymmetric Catalysis*; Morrison, J. D., Ed.; Academic Press: New York, 1985; Vol. 5, pp 1–339.

(3) Whitesell, J. K. C_2-Symmetry and Asymmetric Induction. *Chem. Rev.* **1989**, *89*, 1581–1615.

(4) Trost, B. M. Designing a Receptor for Molecular Recognition in a Catalytic Synthetic Reaction: Allylic Alkylation. *Acc. Chem. Res.* **1996**, *29*, 355–364.

(5) Trost, B. M.; Machacek, M. R.; Aponick, A. Predicting the Stereochemistry of Diphenylphosphino Benzoic Acid (DPPBA)-Based Palladium-Catalyzed Asymmetric Allylic Alkylation Reactions: A Working Model. *Acc. Chem. Res.* **2006**, *39*, 747–760.

(6) Hegedus, L. S. *Transition Metals in the Synthesis of Complex Organic Molecules*, 2nd ed.; University Science Books: Sausalito, CA, 1999.

(7) Blochl, P. E.; Togni, A. First-Principles Investigation of Enantioselective Catalysis: Asymmetric Allylic Amination with Pd Complexes Bearing P,N-Ligands. *Organometallics* **1996**, *15*, 4125–4132.

(8) Johnson, J. S.; Evans, D. A. Chiral Bis(oxazoline) Copper(II) Complexes: Versatile Catalysts for Enantioselective Cycloaddition, Aldol, Michael, and Carbonyl Ene Reactions. *Acc. Chem. Res.* **2000**, *33*, 325–335.

(9) Jørgensen, K. A.; Johannsen, M.; Yao, S.; Audrain, H.; Thorhauge, J. Catalytic Asymmetric Addition Reactions of Carbonyls. A Common Catalytic Approach. *Acc. Chem. Res.* **1999**, *32*, 605–613.

(10) Pfaltz, A. Chiral Semicorrins and Related Nitrogen Heterocycles as Ligands in Asymmetric Catalysis. *Acc. Chem. Res.* **1993**, *26*, 339–345.

(11) Evans, D. A.; Woerpel, K. A.; Hinman, M. M.; Faul, M. M. Bis(oxazolines) as Chiral Ligands in Metal-Catalyzed Asymmetric Reactions: Catalytic Asymmetric Cyclopropanation of Olefins. *J. Am. Chem. Soc.* **1991**, *113*, 726–728.

(12) Fritschi, H.; Leutenegger, U.; Pfaltz, A. Semicorrin Metal-Complexes as Enantioselective Catalysts. 2. Enantioselective Cyclopropane Formation from Olefins with Diazo-Compounds Catalyzed by Chiral (Semicorrinato) Copper Complexes. *Helv. Chim. Acta* **1988**, *71*, 1553–1565.

(13) Evans, D. A.; Faul, M. M.; Bilodeau, M. T.; Anderson, B. A.; Barnes, D. M. Bis(oxazoline) Copper-Complexes as Chiral Catalysts for the Enantioselective Aziridination of Olefins. *J. Am. Chem. Soc.* **1993**, *115*, 5328–5329.

(14) Evans, D. A.; Miller, S. J.; Lectka, T. Bis(oxazoline) Copper(II) Complexes as Chiral Catalysts for the Enantioselective Diels–Alder Reaction. *J. Am. Chem. Soc.* **1993**, *115*, 6460–6461.

(15) Evans, D. A.; Miller, S. J.; Lectka, T.; von Matt, P. Chiral Bis(oxazoline)copper(II) Complexes as Lewis Acid Catalysts for the Enantioselective Diels–Alder Reaction. *J. Am. Chem. Soc.* **1999**, *121*, 7559–7573.

(16) Evans, D. A.; Rovis, T.; Kozlowski, M. C.; Tedrow, J. S. C_2-Symmetric Cu(II) Complexes as Chiral Lewis Acids. Catalytic Enantioselective Michael Addition of Silylketene Acetals to Alkylidene Malonates. *J. Am. Chem. Soc.* **1999**, *121*, 1994–1995.

(17) Evans, D. A.; Burgey, C. S.; Paras, N. A.; Vojkovsky, T.; Tregay, S. W. C_2-Symmetric Copper(II) Complexes as Chiral Lewis Acids. Enantioselective Catalysis of the Glyoxylate–Ene Reaction. *J. Am. Chem. Soc.* **1998**, *120*, 5824–5825.

(18) Hathaway, B. J. In *Comprehensive Coordination Chemistry*, Wilkinson, G., Ed.; Pergamon: New York, 1987; Vol. 5, pp 533–774.

(19) Evans, D. A.; Barnes, D. M.; Johnson, J. S.; Lectka, T.; von Matt, P.; Miller, S. J.; Murry, J. A.; Norcross, R. D.; Shaughnessy, E. A.; Campos, K. R. Bis(oxazoline) and Bis(oxazolinyl)pyridine Copper Complexes as Enantioselective Diels–Alder Catalysts: Reaction Scope and Synthetic Applications. *J. Am. Chem. Soc.* **1999**, *121*, 7582–7594.

(20) Evans, D. A.; Kozlowski, M. C.; Tedrow, J. S. Cationic Bis(oxazoline) and Pyridyl-bis(oxazoline)Cu(II) and Zn(II) Lewis Acid Catalysts. A Comparative Study in Catalysis of Diels–Alder and Aldol Reactions. *Tetrahedron Lett.* **1996**, *37*, 7481–7484.

(21) Corey, E. J.; Imai, N.; Zhang, H. Y. Designed Catalyst for Enantioselective Diels–Alder Addition from a C_2-Symmetric Chiral Bis(oxazoline)-Iron(III) Complex. *J. Am. Chem. Soc.* **1991**, *113*, 728–729.

(22) Tsuji, J.; Minami, I. New Synthetic Reactions of Allylalkyl Carbonates, Allyl Beta-Keto Carboxylates, and Allyl Vinylic Carbonates Catalyzed by Palladium Complexes. *Acc. Chem. Res.* **1987**, *20*, 140–145.

(23) Trost, B. M. Cyclizations via Palladium-Catalyzed Allylic Alkylations. *Angew. Chem., Int. Ed. Engl.* **1989**, *28*, 1173–1192.

(24) Yoon, T. P.; Jacobsen, E. N. Privileged Chiral Catalysts. *Science* **2003**, *299*, 1691–1693.

(25) Meca, L.; Reha, D.; Havlas, Z. Racemization Barriers of 1,1′-Binaphthyl and 1,1′-Binaphthalene-2,2′-diol: A DFT Study. *J. Org. Chem.* **2003**, *68*, 5677–5680.

(26) Kyba, E. P.; Gokel, G. W.; De Jong, F.; Koga, K.; Sousa, L. R.; Siegel, M. G.; Kaplan, L.; Sogah, G. D. Y.; Cram, D. J. Host–guest Complexation. 7. The Binaphthyl Structural Unit in Host Compounds. *J. Org. Chem.* **1977**, *42*, 4173–4184.

(27) Rosini, C.; Franzini, L.; Raffaelli, A.; Salvadori, P. Synthesis and Applications of Binaphthylic C_2-Symmetric Derivatives as Chiral Auxiliaries in Enantioselective Reactions. *Synthesis* **1992**, 503–505.

(28) Pu, L. 1,1′-Binaphthyl Dimers, Oligomers, and Polymers: Molecular Recognition, Asymmetric Catalysis, and New Materials. *Chem. Rev.* **1998**, *98*, 2405–2494.

(29) Shibasaki, M.; Yoshikawa, N. Lanthanide Complexes in Multifunctional Asymmetric Catalysis. *Chem. Rev.* **2002**, *102*, 2187–2219.

(30) Aspinall, H. C.; Greeves, N. Defining Effective Chiral Binding Sites at Lanthanides: Highly Enantioselective Reagents and Catalysts from Binaphtholate and PyBox Ligands. *J. Organomet. Chem.* **2002**, *647*, 151–157.

(31) Chen, Y.; Yekta, S.; Yudin, A. K. Modified BINOL Ligands in Asymmetric Catalysis. *Chem. Rev.* **2003**, *103*, 3155–3212.
(32) Brown, S. N.; Chu, E. T.; Hull, M. W.; Noll, B. C. Electronic Dissymmetry in Chiral Recognition. *J. Am. Chem. Soc.* **2005**, *127*, 16010–16011.
(33) Kelly, R. T.; Whiting, A.; Chandrakumar, N. S. A Rationally Designed, Chiral Lewis Acid for the Asymmetric Induction of Some Diels–Alder Reactions. *J. Am. Chem. Soc.* **1986**, *108*, 3510–3512.
(34) Wipf, P.; Jung, J.-K. Formal Total Synthesis of (+)-Diepoxin σ. *J. Org. Chem.* **2000**, *65*, 6319–6337.
(35) Bochmann, M. Cationic Group 4 Metallocene Complexes and Their Role in Polymerisation Catalysis: The Chemistry of Well Defined Ziegler Catalysts. *J. Chem. Soc., Dalton Trans.* **1996**, 255–270.
(36) Hoveyda, A. H.; Morken, J. P. Enantioselective C–C and C–H Bond Formation Mediated or Catalyzed by Chiral EBTHI Complexes of Titanium and Zirconium. *Angew. Chem., Int. Ed. Engl.* **1996**, *35*, 1262–1284.
(37) Wild, F. R. W. P.; Zsolnai, L.; Huttner, G.; Brintzinger, H.-H. *ansa*-Metallocene Derivatives IV. Synthesis and Molecular Structures of Chiral *ansa*-Titanocene Derivatives with Bridged Tetrahydroindenyl Ligands. *J. Organomet. Chem.* **1982**, *232*, 233–247.
(38) Verdaguer, X.; Lange, U. E. W.; Reding, M. T.; Buchwald, S. L. Highly Enantioselective Imine Hydrosilylation Using (*S*,*S*)-Ethylenebis(5-tetrahydroindenyl)titanium Difluoride. *J. Am. Chem. Soc.* **1996**, *118*, 6784–6785.
(39) Verdaguer, X.; Lange, U. E. W.; Buchwald, S. L. Amine Additives Greatly Expand the Scope of Asymmetric Hydrosilylation of Imines. *Angew. Chem., Int. Ed. Engl.* **1998**, *37*, 1103–1107.
(40) Willoughby, C. A.; Buchwald, S. L. Asymmetric Titanocene-Catalyzed Hydrogenation of Imines. *J. Am. Chem. Soc.* **1992**, *114*, 7562–7564.
(41) Willoughby, C. A.; Buchwald, S. L. Synthesis of Highly Enantiomerically Enriched Cyclic Amines by the Catalytic Asymmetric Hydrogenation of Cyclic Imines. *J. Org. Chem.* **1993**, *58*, 7627–7629.
(42) Yun, J.; Buchwald, S. L. Efficient Kinetic Resolution in the Asymmetric Hydrosilylation of Imines of 3-Substituted Indanones and 4-Substituted Tetralones. *J. Org. Chem.* **2000**, *65*, 767–774.
(43) Hansen, M. C.; Buchwald, S. L. A Method for the Asymmetric Hydrosilylation of *N*-Aryl Imines. *Org. Lett.* **2000**, *2*, 713–715.
(44) Woo, H. G.; Tilley, T. D. Dehydrogenative Polymerization of Silanes to Polysilanes by Zirconocene and Hafnocene Catalysts. A New Polymerization Mechanism. *J. Am. Chem. Soc.* **1989**, *111*, 8043–8044.
(45) Knowles, W. S. Asymmetric Hydrogenation. *Acc. Chem. Res.* **1983**, *16*, 106–112.
(46) Knowles, W. S.; Sabacky, M. J.; Vineyard, B. D. Catalytic Asymmetric Hydrogenation. *J. Chem. Soc., Chem. Commun.* **1972**, 10–11.
(47) Dang, T. P.; Kagan, H. B. The Asymmetric Synthesis of Hydratropic Acid and Amino-Acids by Homogeneous Catalytic Hydrogenation. *J. Chem. Soc., Chem. Commun.* **1971**, 481–482.
(48) Miyashita, A.; Yasuda, A.; Takaya, H.; Toriumi, T.; Ito, K.; Souchi, T.; Noyori, R. Synthesis of 2,2′-Bis(diphenylphosphino)-1,1′-Binaphthyl (BINAP), an Atropisomeric Chiral Bis(triaryl)phosphine, and its use in the Rhodium(I)-Catalyzed Asymmetric Hydrogenation of α-(Acylamino)acrylic Acids. *J. Am. Chem. Soc.* **1980**, *102*, 7932–7934.
(49) Noyori, R.; Ohkuma, T. Asymmetric Catalysis by Architectural and Functional Molecular Engineering: Practical Chemo- and Stereoselective Hydrogenation of Ketones. *Angew. Chem., Int. Ed. Engl.* **2001**, *40*, 40–73.
(50) Noyori, R.; Yamakawa, M.; Hashiguchi, S. Metal–Ligand Bifunctional Catalysis: A Nonclassical Mechanism for Asymmetric Hydrogen Transfer Between Alcohols and Carbonyl Compounds. *J. Org. Chem.* **2001**, *66*, 7931–7944.
(51) Ohta, T.; Takaya, H.; Noyori, R. Bis(diarylphosphino)-1,1′-Binaphthyl BINAP-Ruthenium(II) Dicarboxylate Complexes: New, Highly Efficient Catalysts for Asymmetric Hydrogenations. *Inorg. Chem.* **1988**, *27*, 566–569.
(52) Noyori, R. *Asymmetric Catalysis in Organic Synthesis;* Wiley: New York, 1994.
(53) Hao, J.; Hatano, M.; Mikami, K. Chiral Palladium(II)-Catalyzed Asymmetric Glyoxylate–Ene Reaction: Alternative Approach to the Enantioselective Synthesis of α-Hydroxy Esters. *Org. Lett.* **2000**, *3*, 4059–4062.
(54) Morton, D. A. V.; Orpen, A. G. Structural Systematics 4. Conformations of the Diphosphine Ligands in $M_2(Ph_2PCH_2PPh_2)$ and $M(Ph_2PCH_2CH_2PPh_2)$ Complexes. *J. Chem. Soc., Dalton Trans.* **1992**, 641–653.
(55) Brunner, H.; Winter, A.; Breu, J. Enantioselective Catalysis Part 114. Chirostructural Analysis of Bis(diphenylphosphanyl)ethane Transition Metal Chelates. *J. Organomet. Chem.* **1998**, *553*, 285–306.
(56) Noyori, R.; Takaya, H. BINAP: An Efficient Chiral Element for Asymmetric Catalysis. *Acc. Chem. Res.* **1990**, *23*, 345–350.
(57) Ashby, M. T.; Halpern, J. Kinetics and Mechanism of Catalysis of the Asymmetric Hydrogenation of α,β-Unsaturated Carboxylic Acids by Bis(carboxylato) [2,2′-bis(diphenylphosphino)-1,1′-binaphthyl] ruthenium(II), [RuII(BINAP) $(O_2CR)_2$]. *J. Am. Chem. Soc.* **1991**, *113*, 589–594.
(58) Noyori, R.; Tokunaga, M.; Kitamura, M. Stereoselective Organic Synthesis via Dynamic Kinetic Resolution. *Bull. Chem. Soc. Jpn.* **1995**, *68*, 36–56.
(59) Kitamura, M.; Ohkuma, T.; Inoue, S.; Sayo, N.; Kumobayashi, H.; Akutagawa, S.; Ohta, T.; Takaya, H.; Noyori, R. Homogeneous Asymmetric Hydrogenation of Functionalized Ketones. *J. Am. Chem. Soc.* **1988**, *110*, 629–631.
(60) Halpern, J. Mechanism and Stereoselectivity of Asymmetric Hydrogenation. *Science* **1982**, *217*, 401–407.
(61) Landis, C. R.; Halpern, J. Asymmetric Hydrogenation of Methyl (Z)-α-Acetamidocinnamate Catalyzed by [1,2-Bis(phenyl-o-anisoyl)phosphinoethane] rhodium(I): Kinetics, Mechanism and Origin of Enantioselection. *J. Am. Chem. Soc.* **1987**, *109*, 1746–1754.
(62) Barnhart, R. W.; Wang, X.; Noheda, P.; Bergens, S. H.; Whelan, J.; Bosnich, B. Asymmetric Catalysis. Asymmetric Catalytic Intramolecular Hydroacylation of 4-Pentenals Using Chiral Rhodium

Diphosphine Catalysts. *J. Am. Chem. Soc.* **1994**, *116*, 1821–1830.
(63) Taura, Y.; Tanaka, M.; Funakoshi, K.; Sakai, K. Asymmetric Cyclization Reactions by Rh(I) with Chiral Ligands. *Tetrahedron Lett.* **1989**, *30*, 6349–6352.
(64) Taura, Y.; Tanaka, M.; Wu, X.-M.; Funakoshi, K.; Sakai, K. Asymmetric Cyclization Reactions. Cyclization of Substituted 4-Pentenals into Cyclopentanone Derivatives by Rhodium(I) with Chiral Ligands. *Tetrahedron* **1991**, *47*, 4879–4888.
(65) Wu, X.-M.; Funakoshi, K.; Sakai, K. Highly Enantioselective Cyclization Using Cationic Rh(I) with Chiral Ligands. *Tetrahedron Lett.* **1992**, *33*, 6331–6334.
(66) Bosnich, B. In *Encyclopedia of Inorganic Chemistry*; King, R. B., Ed.; Wiley: New York, 1994; 219–236.
(67) Fairlie, D. P.; Bosnich, B. Homogeneous Catalysis. Mechanism of Catalytic Hydroacylation: The Conversion of 4-Pentenals to Cyclopentanones. *Organometallics* **1988**, *7*, 946–954.
(68) Fairlie, D. P.; Bosnich, B. Homogeneous Catalysis. Conversion of 4-Pentenals to Cyclopentanones by Efficient Rhodium-Catalyzed Hydroacylation. *Organometallics* **1988**, *7*, 936–945.
(69) Ball, R. G.; Payne, N. C. Chiral Phosphine Ligands in Asymmetric Synthesis. Molecular Structure and Absolute Configuration of (1,5-Cyclooctadiene)-(2*S*,3*S*)-2,3-bis(diphenylphosphino)butanerhodium(I) Perchlorate Tetrahedrofuran Solvate. *Inorg. Chem.* **1977**, *16*, 1187–1191.
(70) Fryzuk, M. D.; Bosnich, B. Asymmetric Synthesis. Production of Optically Active Amino Acids by Catalytic Hydrogenation. *J. Am. Chem. Soc.* **1977**, *99*, 6262–6267.
(71) Seebach, D.; Beck, A. K.; Heckel, A. TADDOLs, Their Derivatives, and TADDOL Analogues: Versatile Chiral Auxiliaries. *Angew. Chem., Int. Ed. Engl.* **2001**, *40*, 92–138.
(72) Bradley, D. C.; Mehrotra, R. C.; Rothwell, I. P.; Singh, A. *Alkoxo and Aryloxo Derivatives of Metals*; Academic Press: New York, 2001.
(73) Seebach, D.; Plattner, D. A.; Beck, A. K.; Wang, Y. M.; Hunziker, D.; Petter, W. On The Mechanism of Enantioselective Reactions Using α, α, α′, α′-Tetraaryl-1,3-dioxolane-4,5-dimethanol(TADDOL)-Derived Titanates—Differences Between C_2-Symmetrical and C_1-Symmetrical TADDOLs: Facts, Implications and Generalizations. *Helv. Chim. Acta* **1992**, *75*, 2171–2209.
(74) Gothelf, K. V.; Hazzel, R., G; Jørgensen, K. A. Crystal Structure of a Chiral Titanium-Catalyst–Alkene Complex. The Intermediate in the Catalytic Asymmetric Diels–Alder and 1,3-Dipolar Cycloaddition Reactions. *J. Am. Chem. Soc.* **1995**, *117*, 4435–4436.
(75) Braun, M. The "Magic" Diarylhydroxylmethyl Group. *Angew. Chem., Int. Ed. Engl.* **1996**, *35*, 519–522.
(76) Weber, B.; Seebach, D. Ti-TADDOLate-Catalyzed, Highly Enantioselective Addition of Alkyl- and Aryl-Titanium Derivatives to Aldehydes. *Tetrahedron* **1994**, *50*, 7473–7484.
(77) Seebach, D.; Beck, A. K.; Schmidt, B.; Wang, Y. M. Enantio- and Diastereoselective Titanium-TADDOLate Catalyzed Addition of Diethyl and Bis(3-buten-1-yl) Zinc to Aldehydes. A Full Account with Preparative Details. *Tetrahedron* **1994**, *50*, 4363–4384.
(78) Seebach, D.; Beck, A. K.; Roggo, S.; Wonnacott, A. Chiral Alkoxytitanium(IV) Complexes for Enantioselective Nucleophilic Additions to Aldehydes and as Lewis Acids in Diels–Alder Reactions. *Chem. Ber.* **1985**, *118*, 3673–3682.
(79) Narasaka, K.; Iwasawa, N.; Inoue, M.; Yamada, T.; Kakashima, M.; Sugimori, J. Asymmetric Diels–Alder Reaction Catalyzed by a Chiral Titanium Reagent. *J. Am. Chem. Soc.* **1989**, *111*, 5340–5345.
(80) Gothelf, K. V.; Jørgensen, K. A. On the Mechanism of Ti-TADDOLate-Catalyzed Asymmetric Diels–Alder Reactions. *J. Org. Chem.* **1995**, *60*, 6847–6851.
(81) Gothelf, K. V.; Jørgensen, K. A. On the *trans-cis* Controversy in Ti-TADDOLate-Catalysed Cycloadditions. Experimental Indications for the Structure of the Reactive Catalyst–Substrate Intermediate. *J. Chem. Soc., Perkin Trans.1* **1997**, 111–116.
(82) Haase, C.; Sarko, C. R.; DiMare, M. TADDOL-Based Titanium Catalysts and Their Adducts: Understanding Asymmetric Catalysis of Diels–Alder Reactions. *J. Org. Chem.* **1995**, *60*, 1777–1787.
(83) Seebach, D.; Dahinden, R.; Marti, R. E.; Beck, A. K.; Plattner, D. A.; Kühnle, F. N. M. On the Ti-TADDOLate-Catalyzed Diels–Alder Addition of 3-Butenoyl-1,3-oxazolidine-2-one to Cyclopentadiene. General Features of Ti-BINOLate and Ti-TADDOLate-Mediated Reactions. *J. Org. Chem.* **1995**, *60*, 1788–1799.
(84) García, J. I.; Martinez-Merino, V.; Mayoral, J. A. Quantum Chemical Insights into the Mechanism of the TADDOL-$TiCl_2$ Catalyzed Diels–Alder Reactions. *J. Org. Chem.* **1998**, *63*, 2321–2324.
(85) Seeman, J. I. Effect of Conformational Change on Reactivity in Organic Chemistry. Evaluations, Applications, and Extensions of Curtin–Hammett–Winstein-Holness Kinetics. *Chem. Rev.* **1983**, *83*, 83–134.
(86) Muñiz, K.; Bolm, C. Configurational Control in Stereochemically Pure Ligands and Metal Complexes for Asymmetric Catalysis. *Chem. Eur. J.* **2000**, *6*, 2309–2316.
(87) Mimoun, H.; Yves de Saint Laumer, J.; Giannini, L.; Scopelliti, R.; Floriani, C. Enantioselective Reduction of Ketones by Polymethylhydrosiloxane in the Presence of Chiral Zinc Catalysts. *J. Am. Chem. Soc.* **1999**, *121*, 6158–6166.
(88) Mastranzo, V. M.; Quintero, L.; Anaya de Parrodi, C.; Juaristi, E.; Walsh, P. J. Use of Diamines Containing the α-Phenylethyl Group as Chiral Ligands in the Asymmetric Hydrosilylation of Prochiral Ketones. *Tetrahedron* **2004**, *60*, 1781–1789.
(89) Takahashi, H.; Kawakita, T.; Ohno, M.; Yoshioka, M.; Kobayashi, S. A Catalytic Enantioselective Reaction Using a C_2-Symmetric Disulfonamide as a Chiral Ligand: Alkylation of Aldehydes Catalyzed by Disulfonamide-Ti(O-*i*-Pr)$_4$-Dialkylzinc Reagents. *Tetrahedron* **1992**, *48*, 5691–5700.
(90) Takahashi, H.; Kawakita, T.; Yoshioka, M.; Kobayashi, S.; Ohno, M. Enantioselective Alkylation of Aldehyde Catalyzed by Bissulfonamide-Ti(O-*i*-Pr)$_4$-Dialkylzinc System. *Tetrahedron Lett.* **1989**, *30*, 7095–7098.
(91) Knochel, P.; Jones, P. *Organozinc Reagents*; Oxford University Press: New York, 1999.
(92) Ostwald, R.; Chavant, P.-Y.; Stadtmuller, H.; Knochel, P. Catalytic Asymmetric Addition of

Polyfunctional Dialkylzincs to β-Stannylated and β-Silylated Unsaturated Aldehydes. *J. Org. Chem.* **1994**, *59*, 4143–4153.

(93) Pritchett, S.; Woodmansee, D. H.; Gantzel, P.; Walsh, P. J. Synthesis and Crystal Structures of Bis(sulfonamide) Titanium Bis(alkoxide) Complexes: Mechanistic Implications in the Bis(sulfonamide) Catalyzed Asymmetric Addition of Dialkylzinc Reagents to Aldehydes. *J. Am. Chem. Soc.* **1998**, *120*, 6423–6424.

(94) Pritchett, S.; Gantzel, P.; Walsh, P. J. Synthesis and Structural Study of Titanium Bis(sulfonamido) Bis(amide) Complexes. *Organometallics* **1999**, *18*, 823–831.

(95) Royo, E.; Betancort, J. M.; Davis, T. J.; Walsh, P. J. Synthesis, Structure and Catalytic Properties of Bis[bis(sulfonamido)] Titanium Complexes. *Organometallics* **2000**, *19*, 4840–4851.

(96) Armistead, L. T.; White, P. S.; Gagné, M. R. Synthesis and Structure of Titanium(IV) Amido Complexes Containing C_2-Symmetric Bis(sulfonamide) Ligands. *Organometallics* **1998**, *17*, 216–220.

(97) Pritchett, S.; Woodmansee, D. H.; Davis, T. J.; Walsh, P. J. Improved Methodology for the Asymmetric Alkylation of Aldehydes Employing Bis(sulfonamide) Complexes. *Tetrahedron Lett.* **1998**, *39*, 5941–5944.

(98) Evans, D. A.; Nelson, S. G. Chiral Magnesium Bis(sulfonamide) Complexes as Catalysts for the Merged Enolization and Enantioselective Amination of *N*-Acyloxazolidinones. A Catalytic Approach to the Synthesis of Arylglycines. *J. Am. Chem. Soc.* **1997**, *119*, 6452–6453.

(99) Takahashi, H.; Yoshioka, M.; Ohno, M.; Kobayashi, S. A Catalytic Enantioselective Reaction Using a C_2-symmetric Disulfonamide as a Chiral Ligand: Cyclopropanation of Allylic Alcohols by the Et_2Zn–CH_2I_2–Disulfonamide System. *Tetrahedron Lett.* **1992**, *33*, 2575–2578.

(100) Takahashi, H.; Yoshioka, M.; Shibasaki, M.; Ohno, M.; Imai, N.; Kobayashi, S. A Chiral Enantioselective Reaction Using a C_2-Symmetric Disulfonamide as a Chiral Ligand: Simmons–Smith Cyclopropanation of Allylic Alcohols by the Et_2Zn–CH_2I_2–Disulfonamide System. *Tetrahedron* **1995**, *51*, 12013–12026.

(101) Denmark, S. E.; O'Connor, S. P. Enantioselective Cyclopropanation of Allylic Alcohols. The Effect of Zinc Iodide. *J. Org. Chem.* **1997**, *62*, 3390–3401.

(102) Denmark, S. E.; O'Connor, S. P. Catalytic, Enantioselective Cyclopropanation of Allylic Alcohols. Substrate Generality. *J. Org. Chem.* **1997**, *62*, 584–594.

(103) Corey, E. J.; Sarshar, S.; Lee, D.-H. First Example of a Highly Enantioselective Catalytic Diels–Alder Reaction of an Achiral C_{2v}-Symmetric Dienophile and an Achiral Diene. *J. Am. Chem. Soc.* **1994**, *116*, 12089–12090.

(104) Ichiyanagi, T.; Shimizu, M.; Fujisawa, T. Enantioselectie Diels–Alder Reaction Using Chiral Mg Complexes Derived from Chiral 2-[2-[(Alkyl- or 2-[2-[(Arylsulfonyl)amino]phenyl]-4-phenyl-1,3-oxazoline. *J. Org. Chem.* **1997**, *62*, 7937–7941.

(105) Denmark, S. E.; O'Connor, S. P.; Wilson, S. R. Solution and Solid-State Studies of a Chiral Zinc-Sulfonamide Relevant to an Enantioselective Cyclopropanation Reaction. *Angew. Chem., Int. Ed. Engl.* **1998**, *37*, 1149–1151.

(106) Evans, D. A.; Campos, K. R.; Tedrow, J. S.; Michael, F. E.; Gagné, M. R. Application of Chiral Mixed Phosphorus/Sulfur Ligands to Palladium-Catalyzed Allylic Substitutions. *J. Am. Chem. Soc.* **2000**, *122*, 7905–7920.

(107) Evans, D. A.; Campos, K. R.; Tedrow, J. S.; Michael, F. E.; Gagné, M. R. Chiral Mixed Phosphorus/Sulfur Ligands for Palladium-Catalyzed Allylic Alkylations and Aminations. *J. Org. Chem.* **1999**, *64*, 2994–2995.

(108) Evans, D. A.; Michael, F. E.; Tedrow, J. S.; Campos, K. R. Application of Chiral Mixed Phosphorus/Sulfur Ligands to Enantioselective Rhodium-Catalyzed Dehydroamino Acid Hydrogenation and Ketone Hydrosilylation Processes. *J. Am. Chem. Soc.* **2003**, *125*, 3534–3543.

(109) Barbaro, P.; Currao, A.; Herrmann, J.; Nesper, R.; Pregosin, P. S.; Salzmann, R. Chiral P,S-Ligands Based on D-Thioglucose Tetraacetate. Palladium(II) Complexes and Allylic Alkylation. *Organometallics* **1996**, *15*, 1879–1888.

(110) Brown, J. M.; Evans, P. Structure and Reactivity in Asymmetric Hydrogenation; a Molecular Graphics Analysis. *Tetrahedron* **1988**, *4*, 4905–4916.

(111) Sibi, M. P.; Zhang, R.; Manyem, S. A New Class of Modular Chiral Ligands with Fluxional Groups. *J. Am. Chem. Soc.* **2003**, *125*, 9306–9307.

(112) von Zelewsky, A. *Stereochemistry of Coordination Compounds*; Wiley: New York, 1996.

(113) Brunner, H. Optically Active Organometallic Compounds of Transition Elements with Chiral Metal Atoms. *Angew. Chem. Int., Ed. Engl.* **1999**, *38*, 1194–1208.

(114) Faller, J. W.; Parr, J. Utility of Osmium(II) in the Catalysis of Asymmetric Diels–Alder Reactions. *Organometallics* **2001**, *20*, 697–699.

(115) Faller, J. W.; Grimmond, B. J.; D'Alliessi, D. G. An Application of Electronic Asymmetry to Highly Enantioselective Catalytic Diels–Alder Reactions. *J. Am. Chem. Soc.* **2001**, *123*, 2525–2529.

(116) Babin, J. E.; Whiteker, G. T. U.S. Patent 5,360,938, *Chem. Abstr.* **1994**, *122*, 18660.

(117) Nozaki, K.; Sakai, N.; Nanno, T.; Higashijima, T.; Mano, S.; Horiuchi, T.; Takaya, H. Highly Enantioselective Hydroformylation of Olefins Catalyzed by Rhodium(I) Complexes of New Chiral Phosphine-Phosphite Ligands. *J. Am. Chem. Soc.* **1997**, *119*, 4413–4423.

(118) Reetz, M. T.; Neugebauer, T. New Diphosphite Ligands for Catalytic Asymmetric Hydrogenation: The Crucial Role of Conformationally Enantiomeric Diols. *Angew. Chem., Int. Ed. Engl.* **1999**, *38*, 179–181.

(119) Imai, Y.; Zhang, W.; Kida, T.; Nakatsuji, Y.; Ikeda, I. Diphenylphosphinooxazoline Ligands with a Chiral Binaphthyl Backbone for Pd-Catalyzed Allylic Alkylation. *Tetrahedron Lett.* **1998**, *39*, 4343–4346.

(120) Zhang, W.; Xie, F.; Yoshinaga, H.; Kida, T.; Nakatsuji, Y.; Ikeda, I. A Novel Axially Chiral Phosphine-Oxazoline Ligand with an Axis-Unfixed Biphenyl Backbone: Preparation, Complexation, and Application in an Asymmetric Catalytic Reaction. *Synlett* **2006**, 1185–1188.

(121) Superchi, S.; Casarini, D.; Laurita, A.; Bavoso, A.; Rosini, C. Induction of a Preferred Twist in a Biphenyl Core by Stereogenic Centers: A Novel Approach to the Absolute Configuration of 1,2- and

1,3-Diols. *Angew. Chem., Int. Ed. Engl.* **2001**, *40*, 451–454.
(122) Isaksson, R.; Rashidi-Ranjbar, P.; Sandstrom, J. Synthesis and Chromatographic Resolution of Some Chiral Four-Carbon 2,2′-Bridged Biphenyls. Some Unusually High Selectivity Factors. *J. Chem. Soc., Perkin Trans. 1* **1991**, 1147–1152.
(123) Imai, Y.; Zhang, W.; Kida, T.; Nakatsuji, Y.; Ikeda, I. Novel Chiral Bisoxazoline Ligands with a Biphenyl Backbone: Preparation, Complexation, and Application in Asymmetric Catalytic Reactions. *J. Org. Chem.* **2000**, *65*, 3326–3333.
(124) Pastor, S. D.; Shum, S. P.; Rodebaugh, R. K.; Debellis, A. D.; Clarke, F. H. Sterically Congested Phosphite Ligands: Synthesis, Crystallographic Characterization, and Observation of Unprecedented Eight-Bond ^{31}P, ^{31}P Coupling in the ^{31}P-NMR Spectra. *Helv. Chim. Acta* **1993**, *76*, 900–915.
(125) Hartwig, J. Synthetic Chemistry—Recipes for Excess *Nature* **2005**, *437*, 487–488.
(126) Costa, A. M.; Jimeno, C.; Gavenonis, J.; Carroll, P. J.; Walsh, P. J. Optimization of Catalyst Enantioselectivity and Activity Using Achiral and Meso Ligands. *J. Am. Chem. Soc.* **2002**, *124*, 6929–6941.
(127) Mino, T.; Kashihara, K.; Yamashita, M. New Chiral Phosphine-Amide Ligands in Palladium-Catalyzed Asymmetric Allylic Alkylations. *Tetrahedron: Asymmetry* **2001**, *12*, 287–291.
(128) Clayden, J.; Lai, L. W.; Helliwell, M. Using Amide Conformation to "Project" the Stereochemistry of an (–)-Ephedrine-Derived Oxazolidine: A Pair of Pseudoenantiomeric Chiral Amido-Phosphine Ligands. *Tetrahedron: Asymmetry* **2001**, *12*, 695–698.
(129) Brandt, P.; Södergren, M. J.; Andersson, P. G.; Norrby, P.-O. Mechanistic Studies of Copper-Catalyzed Alkene Aziridination. *J. Am. Chem. Soc.* **2000**, *122*, 8013–8020.
(130) Evans, D. A.; Bilodeau, M. T.; Faul, M. M. Development of the Copper-Catalyzed Olefin Aziridination Reaction. *J. Am. Chem. Soc.* **1994**, *116*, 2742–2753.
(131) Li, Z.; Conser, K. R.; Jacobsen, E. N. Asymmetric Alkene Aziridination with Readily Available Chiral Diimine-Based Catalysts. *J. Am. Chem. Soc.* **1993**, *115*, 5326–5327.
(132) Li, Z.; Quan, R. W.; Jacobsen, E. N. Mechanism of the (Diimine)copper-Catalyzed Asymmetric Aziridination of Alkenes. Nitrene Transfer via Ligand-Accelerated Catalysis. *J. Am. Chem. Soc.* **1995**, *117*, 5889–5890.
(133) Sibi, M. P.; Venkatraman, L.; Liu, M.; Jasperse, C. P. A New Approach to Enantiocontrol and Enantioselectivity Amplification: Chiral Relay in Diels–Alder Reactions. *J. Am. Chem. Soc.* **2001**, *123*, 8444–8445.
(134) Sibi, M. P.; Chen, J.; Stanley, L. Enantioselective Diels–Alder Reactions: Effect of the Achiral Template on Reactivity and Selectivity. *Synlett* **2007**, 298–302.